

Maximal Simplification of Polyhedral Reductions

LOUIS NARMOUR, Colorado State University, USA and Univ Rennes, Inria, CNRS, IRISA, France

TOMOFUMI YUKI, Univ Rennes, Inria, France

SANJAY RAJOPADHYE, Colorado State University, USA

Reductions combine multiple input values with an associative operator to produce a single (or multiple) result(s). When the *same* input value contributes to *multiple* outputs, there is an opportunity to *reuse* partial results, enabling *reduction simplification*. Simplification produces a program with lower asymptotic complexity. It is well known that reductions in polyhedral programs may be simplified *automatically* but previous methods are incapable of exploiting all available reuse. This paper resolves this long standing open problem, thereby attaining minimal asymptotic complexity in the simplified program.

CCS Concepts: • **Theory of computation** → **Program analysis**; **Abstraction**; **Program analysis**; • **Software and its engineering** → **Incremental compilers**; **Software performance**; **Incremental compilers**; • **General and reference** → **Performance**.

Additional Key Words and Phrases: polyhedral compilation, algorithmic complexity, program transformation

1 INTRODUCTION

The polyhedral model [Feautrier 1991, 1992a,b; Quinton and Van Dongen 1989; Rajopadhye 1986, 1989; Rajopadhye et al. 1986] is a mathematical formalism for specifying, analyzing and transforming compute- and data-intensive programs. Such programs occur in a wide variety of application domains, like dense linear algebra, signal and image processing, convolutional neural nets, deep learning, back-propagation training, and dynamic programming, to name just a few. The Multi-Level Intermediate Representation [Lattner et al. 2021, 2020] (MLIR) in the LLVM Compiler Infrastructure is largely based on this model.

Reductions and scans—applying an associative (and often commutative) operator to collections of values, to produce one or more results—are ubiquitous in computing. Sixty years ago, Iverson proposed them as high-level programming abstractions in APL [Iverson 1962], and Map-Reduce [Dean and Ghemawat 2008] popularized them on large distributed systems. It is therefore important to develop automatic techniques to implement them efficiently, i.e., to compile high level specifications of reductions automatically, and preferably optimally, especially for machine learning workloads [Xie et al. 2022]. Reductions have long history in the polyhedral model [Gupta et al. 2002; Le Verge 1992a,b; Redon and Feautrier 1994; Roychowdhury 1988], and are now even integral to MLIR.

In this paper, we tackle the problem of optimizing reductions in the polyhedral model. Typical compiler optimizations yield at best a *constant fold* speedup. Since the polyhedral model allows automatic parallelization, this constant can scale with the number of processors, p , but the ideal speedup on p processors is still “just” p -fold. On the other hand, a complexity reduction from, say n^3 to n^2 yields “unbounded” speedup, since asymptotically, n can be arbitrarily large. Gautam and

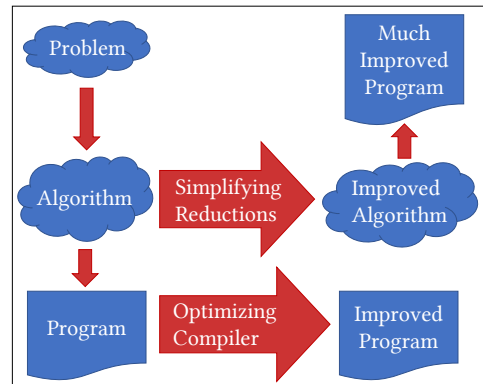


Fig. 1. Simplification improves the asymptotic complexity of the *algorithm*.

Rajopadhye [2006] previously showed how to reduce, by such polynomial degrees, the *asymptotic complexity* of polyhedral reductions. They developed a program transformation called *simplification*, and outlined an algorithm that automatically simplifies polyhedral reductions. Also note that the resulting program remains polyhedral, and can benefit further from automatic parallelization and locality optimizations provided by modern polyhedral compilers.

Example	Asymptotic Complexity		Performance Improvement		
	Original	Simplified	Original	Simplified	Speedup
GMM-GS	$O(N^2 K^2)$	$O(NK)$	29.2ms	4.1 ms	7.1
GMM-MH	$O(N(N + K))$	$O(N)$	0.94 ms	0.72 ms	1.3
GMM-LW	$O(N(N + K))$	$O(N)$	2.5 s	1.7 s	1.5
LDA-GS	$O(W^2 K^2)$	$O(WK)$	timeout	7.1 ms	$> 6.1 \times 10^6$
LDA-MH	$O(W^2 K)$	$O(WK)$	timeout	0.69 s	$> 6.3 \times 10^3$
LDA-LW	$O(W^2 K)$	$O(W)$	timeout	41.1 s	$> 1.1 \times 10^3$
DMM-GS	$O(WADK^2 + D^2 K^2)$	$O((W + A)KD)$	2.2 s	0.54 s	4.1
DMM-MH	$O(D^2 K^2 + D(W + A))$	$O((K + W + A)D)$	529 ms	14.3 ms	37
DMM-LW	$O((WA + K)D)$	$O((K + W + A)D)$	71 s	1.23 s	58
LBP-St	$O(NKD^2)$	$O(NKD)$	16.9 s	15.1 s	1.1
CoxPH	$O(K^2 N^2)$	$O(K^2 N)$	69.1 ms	8.4ms	8.2

Table 1. (from Yang et al. 2021) Impact of simplification on statistical learning applications. Benchmarks include Gaussian Mixture Models (GMM), Latent Dirichlet Allocation (LDA) and Dirichlet Multinomial Mixtures (DMM). Algorithms include Gibbs Sampling (GS), Metropolis Hasting (MH) and Likelihood Weighting (LW). See their paper for details of benchmarks, algorithms, size parameters, machine specs, etc.

Simplification has garnered interest recently. Yang, et al. [2020; 2021] showed its use in many applications drawn from statistical learning and Bayesian inference, which is claimed to be the future of AI/ML (see Table 1). The Gautam and Rajopadhye [2006] algorithm leaves some redundant computation “on the table.” ***Our main contribution is that we show how to attain maximal simplification, thereby producing a program with the minimum asymptotic complexity that can be obtained through reuse-based simplification.*** We illustrate and motivate the issues with a sequence of progressively difficult problems.

EXERCISE 1. Given an input array X of length $2N$, write a program to compute an array $Y[i]$ for $0 \leq i \leq N$, specified by the Equation 1. The final program must have $O(N)$ complexity and improve the naive, quadratic time program shown at the top of Fig. 2.

$$Y[i] = \sum_{j=i}^{2i} X[j] \quad (1)$$

EXERCISE 2. Now replace addition with the max operation and compute with $O(N)$ complexity,

$$Y[i] = \max_{j=i}^{2i} X[j] \quad (2)$$

The following problem is harder still, as it involves a higher dimensional program.

EXERCISE 3. Optimize the $O(N^4)$ program that computes, for $0 \leq i \leq j \leq N$,

$$Y[i, j] = \max_{k=i}^{2i} \max_{l=i+j}^{2j} X[k, l] \quad (3)$$

The final program must have $O(N^2)$ complexity and improve the quartic time program shown at the bottom of Fig. 2.

Exercise 1 can be solved easily by a smart sophomore (see Section 6.1), but Exercise 2 is surprisingly difficult because the (max) operator does not admit an inverse. Such operators are very common in many dynamic programming algorithms. Indeed, *polyadic dynamic programming* [Li and Wah 1985] are nothing but reductions, and are widely used in many bio-informatics algorithms [MAT 2006; Chitsaz et al. 2009a,b; Flamm et al. 2000; Lorenz et al. 2011; Lyngso et al. 1999a,b; Nussinov and Jacobson 1980; Nussinov et al. 1978; Wolfinger et al. 2004; Zadeh et al. 2011; Zuker and Stiegler 1981].

At the heart of our solution is *piece-wise simplification*, the notion that we can split the problem into a number of pieces, and then independently simplify each piece. Such *piece-wise affine transformations*, also known as index-set splitting, have a long history in other polyhedral analyses [Bondhugula et al. 2014; Griebel et al. 2000; Rajopadhye et al. 1992; Vasilache et al. 2007]. The difficulty lies in that in general, there are infinitely many ways in which to split a polyhedron. We give a constructive proof showing how to select a finite number of pieces for simplification.

The remainder of this paper is organized as follows. We review the notation and background material on the polyhedral model, simplification, and its limitations in Section 2. We lay out our assumptions and main claims in Section 3. Then in Sections 4 and 5, respectively, we provide proofs for maximally simplifying general higher dimensional and 2-dimensional reductions. Finally, we give illustrative solutions in Section 6 to the exercises above and conclude in Section 7.

2 NOTATION AND BACKGROUND

Invented over 35 years ago in independent, related threads by Rajopadhye [1986; 1989; 1986] and others [Feautrier 1991, 1992a,b; Fortes and Moldovan 1984; Irigoin and Triolet 1988; Lam 1989; Lengauer 1993; Quinton and Van Dongen 1989], the *polyhedral model* is a mathematical formalism for reasoning about, and mapping with provably optimal transformations, a precisely defined class of computations. It provides the technology to map high level descriptions of compute- and data-intensive programs to a range of highly parallel targets. Polyhedral “programs” are most cleanly viewed as *equations* defined over *polyhedral domains*, evaluating an *expression* at each point therein. Equations are strictly more general than *affine control loops* and may not even be computable [Saouter and Quinton 1993].

2.1 Polyhedra, affine/linear functions, parameters, volume, and asymptotic complexity

A parametric integer polyhedron in \mathbb{Z}^k for some $k \geq 0$ is defined as the intersection of a finite number of half-spaces and it may have one or more designated indices, like N in Exercises 1-3, called size parameters. The polyhedron defined with m inequality constraints, n equality constraints, and q size parameters is written as,

$$\mathcal{D} = \{ z \in \mathbb{Z}^k \mid Az + Bp \geq c; \quad Cz + Dp = d; \} \quad (4)$$

where A is an $m \times k$ matrix, B is an $m \times q$ matrix, z is the k -vector $[i_1, i_2, \dots, i_k]^T$, p is the q -vector $[p_1, p_2, \dots, p_q]^T$, and c is the m -vector $[c_1, c_2, \dots, c_m]^T$. Similarly, C is an $n \times k$ matrix, D is an $n \times q$ matrix, and d is the n -vector $[i_1, i_2, \dots, i_n]^T$. The rows of A and B characterize the coefficients of

```
// Exercise 1
for (i=0; i<=N; i++)
  for (j=i; j<=2*i; j++)
    Y[i] += X[j];
```

```
// Exercise 2
for (i=0; i<=N; i++)
  for (j=i; j<=2*i; j++)
    Y[i] = max(Y[i], X[j]);
```

```
// Exercise 3
for (i=0; i<=N; i++)
  for (j=i; j<=N; j++)
    for (k=i; k<=2*i; k++)
      for (l=i+j; l<=2*j; l++)
        Y[i, j] = max(Y[i, j], X[k, l]);
```

Fig. 2. Quadratic and quartic time programs to compute Exercises 1, 2 and 3.

inequalities for the indices (in z) and parameters (in p) and the rows of C and D characterize the equalities. Typically there is no upper bound on parameters, and a parametric polyhedron may define an unbounded family of polytopes, one for each value of the parameters.¹ The *volume*, cardinality, or the number of integer points, in such a parametric polyhedron is known to be a polynomial function of the parameters [Loechner and Wilde 1997] and this polynomial represents the asymptotic complexity of a program that performs a constant time operation at every point in the polyhedron. Libraries like `isl` [Verdoolaege 2016] provide tools that can automatically deduce such polynomials from polyhedral loop programs. The degree of this polynomial, also called the number of *free dimensions*, or *dimensionality* of the polyhedron, is the number of indices in \mathcal{D} , less the number of its linearly independent equalities (i.e., $k - n$). It is the rank of the smallest linear subspace that spans the polyhedron. In this paper, we assume that our programs have a single size parameter.

For example, consider the 3D polyhedron of points $z = [i, j, k, l] \in \mathbb{Z}^4$ bounded by the following five constraints: (1) $i \leq j$, (2) $j \leq N$, (3) $i \leq k$, (4) $k \leq 2i$, and (5) $l = i + j$. We say that this is 3-dimensional because there are four indices and one equality constraint. To put these constraints in the form of Equation 4, they should really be viewed together as,

$$\begin{aligned} -1i + 1j + 0k + 0l + 0N &\geq 0 \\ 0i - 1j + 0k + 0l + 1N &\geq 0 \\ -1i + 0j + 1k + 0l + 0N &\geq 0 \\ 2i + 0j - 1k + 0l + 0N &\geq 0 \end{aligned}$$

forming A , B , and c , and,

$$-1i - 1j + 0k + 1l + 0N = 0$$

forming C , D , and d . In this example, z is the 4-vector of the indices $[i, j, k, l]^T$ and p is the 1-vector of the size parameters $[N]^T$. A is a 4×4 matrix, B a 4×1 matrix, c a 4-vector, C a 1×4 matrix, D a 1×1 matrix, and d a 1-vector,

$$A = \begin{bmatrix} -1 & 1 & 0 & 0 \\ 0 & -1 & 0 & 0 \\ -1 & 0 & 1 & 0 \\ 2 & 0 & -1 & 0 \end{bmatrix}, B = \begin{bmatrix} 0 \\ 1 \\ 0 \\ 0 \end{bmatrix}, c = \begin{bmatrix} 0 \\ 0 \\ 0 \\ 0 \end{bmatrix}, C = [-1 \quad -1 \quad 0 \quad 1], D = [0], d = [0] \quad (5)$$

Notice that the equality constraint $l = i + k$, together with the fact that l does not appear in the inequalities imply that this is actually a 3-D polyhedron (indeed, a tetrahedron) embedded in a 4-D space. Each row of A is associated with one of the tetrahedron's 2D faces and its coefficients can be interpreted geometrically as the normal vector of the corresponding face. The second row of A , for example, $[0, -1, 0, 0]$ represents the back vertical face in the plane $j = N$ parallel to the ik -plane in Figure 3. The normal vector to this face is the vector pointing along the negative j direction. This notion of child faces and their normal vectors is important in the context of simplification and is discussed more in Section 2.5 where we formalize the face lattice. Notice that this tetrahedron corresponds precisely to *the slice of the domain* of the reduction given in Exercise 3 when $l = i + j$, which should be clear after inspecting the expressions bounding the loop iterators of the code snippet in Figure 2. In other words, the points in the polyhedron formed by Equation 5 represent the set of values that the loop iterators i , j , k , and l can take for the first iteration of the l -loop in Figure 2, because the value of l on the first iteration is $i + j$.

¹We can also simplify parameterized programs/equations where each instance has an unbounded computation. Our results, like those of Gautam and Rajopadhye [2006] are also applicable to such programs.

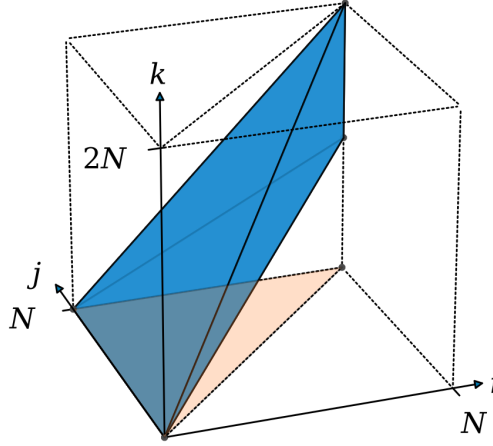


Fig. 3. The tetrahedron defined by constraints in Equation 5. Note that it is embedded in \mathbb{Z}^4 (with $l = i + j$) and the blue region shows the projection onto the ijk -space and the orange region shows the projection on the ij -plane.

In addition to polyhedral sets, viewed as collections of points, we need to describe relations between points. A linear/affine function f is a mapping $\mathbb{Z}^m \rightarrow \mathbb{Z}^n$ given by $z \mapsto Ez + e$, for some $n \times m$ matrix, E , and an n -vector, e . For example, consider the following mapping from $\mathbb{Z}^4 \rightarrow \mathbb{Z}^2$ given by,

$$E = \begin{bmatrix} 1 & 0 & 0 & 0 \\ 0 & 1 & 0 & 0 \end{bmatrix}, \quad e = \begin{bmatrix} 0 \\ 0 \end{bmatrix}$$

Here, every point $[i, j, k, l] \in \mathbb{Z}^4$ is mapped to the point $[i, j] \in \mathbb{Z}^2$. Geometrically, this mapping can be interpreted as a projection onto the ij -plane. Applying this mapping to the tetrahedron defined by Equation 5 gives the bottom orange triangular image shown in Figure 5. Notice that this mapping corresponds precisely to the way in which elements of the reduction body contribute to elements in the output variable Y in Exercise 3 (i.e., each point $[i, j, k, l]$ in the innermost loop accumulates into $Y[i, j]$). This mapping can be expressed as an isl set using “ $\{[i, j, k, l] \rightarrow [i, j]\}$ ”.

2.2 Programs, equations, reductions, accumulation and reuse space

We are interested in analyzing programs like the examples given in Exercises 1-3. Such programs consist of arbitrarily nested loops with affine control and a *single statement* in the body, plus *initialization* statements as appropriate. Each statement accumulates, using the reduction operator (or initializes) some element of an output array. The right-hand side of the statements are *arbitrary expressions* evaluated in constant time, reading other array variables via affine access functions. Our reduction operators are associative *and* commutative, so the execution order of the loops are irrelevant. We can treat every instance of the loop body (for every legal value of the surrounding indices) as a new, dummy variable. With this analysis, we can formalize our program representation as equations of the form,

$$Y[f_p(z)] = \bigoplus_{z \in \mathcal{D}} X[f_r(z)] \quad (6)$$

The affine function f_p on the left-hand side of Equation 6 is called the projection function and it defines how points in the reduction body are mapped to points in the output (i.e., where each

iteration point $z \in \mathcal{D}$ *writes* or *accumulates*). Since reductions combine multiple values to produce multiple answers, f_p is a *rank-deficient* (and therefore a many-to-one) linear *write access*,

$$f_p : \mathbb{Z}^d \rightarrow \mathbb{Z}^{d-a} \quad (7)$$

where $a > 0$. The image of \mathcal{D} by f_p is the set of results produced by the reduction and is the *domain* of Y , denoted by $\mathcal{D}_Y = f_p(\mathcal{D})$. The accumulation space,

$$A = \ker(f_p) \subseteq \mathbb{Z}^k \quad (8)$$

is defined as the null space of the projection function and is an a -dimensional subspace.

The function f_r on the right-hand side of Equation 6 defines how points in the reduction body are mapped to points from the input (i.e., from where each point $z \in \mathcal{D}$ *reads*).

$$f_r : \mathbb{Z}^d \rightarrow \mathbb{Z}^{d-r} \quad (9)$$

The goal of simplification is to analyze the array access functions that occur in the equation/program, identify potential reuse, and therefore replace this body by a variable of fewer free dimensions. Simplification is possible only if the *same* input value is read at multiple points in \mathcal{D} . It is well known [Fortes and Moldovan 1984; Rajopadhye et al. 1986; Wong and Delosme 1988] that this happens if f_r is rank-deficient, i.e., with a non-trivial null space (i.e., when $r > 0$). The points z and z' access the same value of X if and only if $f_r(z) = f_r(z')$, or $z - z'$ is a linear combination of some *basis vectors* of the null space of f_r . Let the null space of f_r be called the *reuse space*, and be denoted by R , where,

$$R = \ker(f_r) \subseteq \mathbb{Z}^r \quad (10)$$

Any vector, $\rho \in R$ constitutes a valid *reuse vector* along which the reduction body can be simplified. We provide a concrete illustration of this in Section 2.3. Gautam and Rajopadhye [2006] provide all the details.

Looking back again at Exercise 3, the domain of the reduction body can be represented as the polyhedral set,

$$\mathcal{D} = \{[i, j, k, l] \mid j \leq N \text{ and } i \leq k \leq 2i \text{ and } i + j \leq l \leq 2j\} \quad (11)$$

From the code snippet in Figure 2, we can see that each point $[i, j, k, l]$ in \mathcal{D} accumulates into the location in Y according to the function, $f_p = \{[i, j, k, l] \rightarrow [i, j]\}$. The accumulation space is the 2D space spanned by the basis vectors $[0, 0, 1, 0]$ and $[0, 0, 0, 1]$ (i.e., along any direction parallel to the kl -plane). Similarly, each point $[i, j, k, l]$ in \mathcal{D} reads from X according to the function $f_r = \{[i, j, k, l] \rightarrow [k, l]\}$. The reuse space is the 2D space spanned by the basis vectors $[1, 0, 0, 0]$ and $[0, 1, 0, 0]$ (i.e., along any direction parallel to the ij -plane).

2.3 Reduction simplification

Consider a simple example: compute an N -element array Y where,

$$Y[i] = \max_{j=0}^i X[i - j] \quad (12)$$

The equation has a reduction with the max operator. The *reduction body* is defined over the domain, $\mathcal{D} = \{[i, j] \mid 0 \leq j \leq i < N\}$, the red triangle in Fig. 4.

The i -th result, $Y[i]$, is the accumulation of the values of the reduction body at points in the i -th column of the triangle. The complexity of the equation is the number of integer points in \mathcal{D} , namely $O(N^2)$. Simplification is possible because the body *exhibits potential reuse along the vector* $\rho = [1, 1]$ (green arrow). Recall that the reuse space defined in Equation 10 is the null space of the indexing expression appearing inside the reduction body, which is $f_d : \{[i, j] \rightarrow [i - j]\}$ in this example. Any two points $[i, j], [i', j'] \in \mathcal{D}$ separated by a scalar multiple of ρ read the same

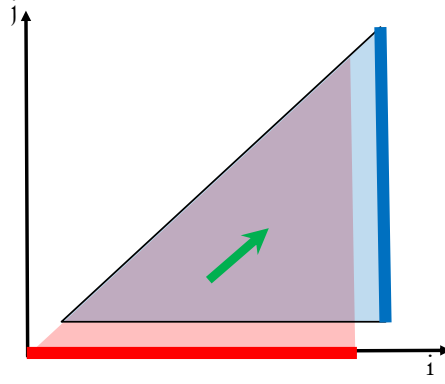


Fig. 4. Simplification of a quadratic equation (computation defined over a triangle) to a linear complexity (the residual computation is defined only over the points in the bottom row).

value of X because $X[i - j] = X[i' - j']$. In other words, the body expression evaluates to the same value at all points along $[1, 1]$. Simplification exploits this reuse to read and compare *only the $O(N)$ distinct values*. A geometric explanation of simplification is:

- translate \mathcal{D} (shift the red triangle) by ρ (green arrow) yielding \mathcal{D}_s (the blue triangle);
- delete all computations in the intersection of the two, leaving
- residual computation on only the facets (here, edges) of \mathcal{D} and/or \mathcal{D}_s .

Additionally, some of these facets can also be removed: the diagonal one, being parallel to ρ was already included in the intersection, and the vertical (blue) one is *external* since it does not contribute to any answer. This leaves a residual computation on only the bottom facet. Thus, we can replace the $O(N^2)$ equation with the following,

$$Y[i] = \begin{cases} i = 0 & : X[i] \\ i > 0 & : \max(Y[i - 1], X[i]) \end{cases}$$

which has only $O(N)$ complexity. Indeed, Equation 12 specifies a simple scan (prefix-max) of the input, albeit in a counter-intuitive manner.

2.4 Recursive Simplification

In the general case, with a d -dimensional reduction body, a -dimensional accumulation and r -dimensional reuse, the above idea is applied recursively, on the face lattice, starting with \mathcal{D} , and at each step we simplify the facets of the current face \mathcal{F} . The face lattice is formally defined in Sec 2.5, but the intuition should be clear.

We first assume that the reduction operator admits an inverse, \ominus . Later, we consider non-invertible operators. The key idea is that exploiting reuse along ρ avoids evaluating e at most points in \mathcal{F} . Specifically, let \mathcal{F}' be the translation of \mathcal{F} along ρ . Then all the computation in $\mathcal{F} \cap \mathcal{F}'$ is avoided, and we only need to consider the two differences $\mathcal{F}' \setminus \mathcal{F}$ and $\mathcal{F} \setminus \mathcal{F}'$, i.e., the union of some of the facets of \mathcal{F} . We are left with *residual computations* defined only on the facets of \mathcal{F} . And indeed, not all the facets are needed (see below).

At each step of the recursion, the asymptotic complexity is reduced by exactly one polynomial degree, because facets of \mathcal{F} have one fewer free index. Furthermore, at each step, the faces saturated by the ancestors ensure that the new ρ is linearly independent of the previously chosen ones. Hence,

the method is optimal—the reduction in asymptotic complexity is by a polynomial whose degree is the number of dimensions of the feasible reuse space of the original domain and all available reuse is fully exploited. This holds regardless of the choice of ρ at any level of the recursion (all roads lead to Rome) even though there are infinitely many choices in general.

However, when the operator does not admit an inverse, the above method does not always work as motivated by Exercise 2. Now, we must formulate the reuse space more carefully with additional constraints, which may reduce the feasible space to the point that simplification is impossible. Before explaining this, we formalize our notation.

2.5 Face lattice of the reduction body

The face lattice [Loechner and Wilde 1997] is an important data structure for simplification. For a polyhedron, \mathcal{D} , it is a graph whose nodes are the *faces* of \mathcal{D} . At the “top” of the lattice is \mathcal{D} itself. Each face is the intersection of \mathcal{D} with one or more *equalities* of the form $\alpha z + \gamma = 0$ obtained by *saturating* one or more of the inequality constraints in \mathcal{D} . The dimensionality of each face is the rank of the smallest linear subspace that spans the face. We refer to each k -dimensional face as a (k) -*face*.

If \mathcal{D} is d -dimensional then a *facet* \mathcal{F} of \mathcal{D} is one of its child $(d - 1)$ -faces. More than one constraint may be saturated, and this yields recursively, facets of facets, or *faces*. In the lattice, faces are arranged level by level, and each face saturates exactly one constraint in addition to those saturated by its “parent.”² Zero-dimensional faces are called *vertices* and 1-dimensional faces are *edges*.

The face lattice of the polyhedron defined by Equation 11 is illustrated in Figure 6 with its five inequality constraints shown again in Figure 5. This is a 4D polyhedron with five 3D faces, ten 2D faces, ten 1D faces (“edges”), and five 0D faces (“vertices”). Each node is labeled with the corresponding indices of the constraints in Figure 5 that, *when saturated*, describe the set of points on the face. The 3D face at node $\{3\}$, for example, is given by Equation 5 and was previously illustrated in Figure 3. The node $\{3\}$ has the four child nodes $\{2, 3\}$, $\{3, 4\}$, $\{1, 3\}$, and $\{0, 3\}$ because the tetrahedron in Figure 3 has four 2D faces. The set describing the points in the 2D face at node $\{2, 3\}$ is,

$$\{z \mid Az + Bp \geq c; Cz + Dp = d;\}$$

where,

$$A = \begin{bmatrix} -1 & 1 & 0 & 0 \\ 0 & -1 & 0 & 0 \\ -1 & 0 & 1 & 0 \end{bmatrix}, B = \begin{bmatrix} 0 \\ 1 \\ 0 \end{bmatrix}, c = \begin{bmatrix} 0 \\ 0 \\ 0 \end{bmatrix}, C = \begin{bmatrix} 2 & 0 & -1 & 0 \\ -1 & -1 & 0 & 1 \end{bmatrix}, D = \begin{bmatrix} 0 \\ 0 \end{bmatrix}, d = \begin{bmatrix} 0 \\ 0 \end{bmatrix} \quad (13)$$

Notice that this set is described by three inequality constraints and two equality constraints.

Let us introduce some notation to refer to a particular face in the lattice. We will impose an ordering on nodes in the face lattice at a particular depth, where the nodes are ordered from left to right. Given a polyhedral set \mathcal{D} , its list of constraints, and its face lattice, let us introduce the following definitions.

Definition 2.1. Let \mathcal{F}_i^k be the i ’th (k) -face in the lattice and be given by the set,

$$\mathcal{F}_i^k = \{z \mid A'z + B'p \geq c'; C'z + D'p = d'\} \quad (14)$$

²Admittedly, the notion of a parent is ambiguous in a lattice, so this is abuse of notation. Our algorithms visit faces recursively in a top down manner, and the call tree of this recursion providee the necessary context.

	Inequality
c_0	$j - N \geq 0$
c_1	$-i + k \geq 0$
c_2	$2i - k \geq 0$
c_3	$-i - j + l \geq 0$
c_4	$2j - l \geq 0$

Fig. 5. Constraints of the polyhedron defined by Equation 11.

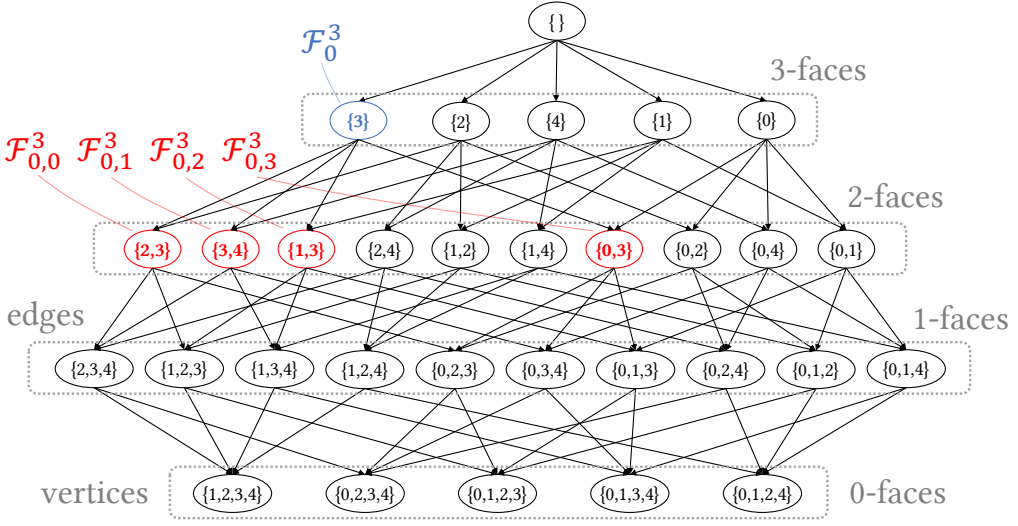


Fig. 6. Face lattice of the polyhedron defined by Equation 11. Each node (oval) is a face of the polyhedron. The numbers in each node indicate the set of saturated constraints from Figure 5 that characterize the face. The node “{3}” for example represents the 3D face $\{[i, j, k, l] : j \leq N \text{ and } i \leq k \leq 2i \text{ and } l = i + j\}$ where the inequality constraint c_3 in Figure 5 is saturated (i.e., treated as an equality constraint). This is the set previously depicted in Figure 3. The blue label \mathcal{F}_0^3 denotes the first (3)-face per Definition 2.1. Its *four* child nodes (the red $\mathcal{F}_{0,j}^3$ labels per Definition 2.2) represent the *four* 2D triangular faces of the tetrahedron in Figure 3.

where the rows of A' , B' , c' , C' , D' , and d' are some permutation of the rows in A , B , c , C , D , and d for \mathcal{D} depending on which constraints are saturated on \mathcal{F}_i^k .

Definition 2.2. Let $\mathcal{F}_{i,j}^k$ be the j 'th child of the i 'th (k)-face in the lattice and be given by the set,

$$\mathcal{F}_{i,j}^k = \{z \in \mathcal{F}_i^k \mid C''z + D''p = d''\} \quad (15)$$

where C'' , D'' , and d'' refer to the *single additionally saturated* constraint relative to \mathcal{F}_i^k . Note that the word *single* only applies when \mathcal{F}_i^k is simplicial (i.e., hyper-triangular). In general, saturating a particular constraint may cause additional constraints to become saturated. Geometrically, this corresponds to the fact that two (k)-faces may only intersect at a ($k - 2$)-face, not at a ($k - 1$)-face. However, simplicial domains have the useful property that the intersection of any (k)-face with any other (k)-face is always a ($k - 1$)-face. This is discussed further in Section 3.

Definition 2.3. Let $v_{i,j}^k$ be the normal vector of the additionally saturated constraint in the j 'th child of the i 'th (k)-face in the lattice and be defined as,

$$v_{i,j}^k = C'' \quad (16)$$

where C'' is the row-vector of the single additionally saturated constraint of $\mathcal{F}_{i,j}^k$.

Definition 2.4. Let \mathcal{H}_i^k be the smallest linear subspace that spans \mathcal{F}_i^k and be given by the unbounded set,

$$\mathcal{H}_i^k = \{z \mid C'z = 0\} \quad (17)$$

containing only equality constraints, one for each saturated constraint. Note that only the *linear* piece over the index (and not the parameter) space of constraints is kept. Although the constraints

are affine, we say in general that any two *parallel* constraints are characterized by the *same* linear subspace. For example, suppose the two (1)-faces $i = 0$ and $i = N$ exist on some (2)-face $\{[i, j]\} \in \mathbb{Z}^2$. We say that the linear space of these two (1)-faces is spanned by the linear basis $[0, 1]$ regardless of *where* each face intersects the i -axis. The C' appearing in Equations 14 and 17 should be understood to have the same values.

For example, in Figure 6, we say that \mathcal{F}_0^3 refers to the first (3)-face (i.e., node $\{3\}$) and its linear subspace \mathcal{H}_0^3 is defined by the set with the coefficients of C' , D' and d' having the values of C , D and d in Equation 5. Similarly, we say that $\mathcal{F}_{0,0}^3$ refers to its *first* child (2)-face (i.e., node $\{2, 3\}$), and its linear subspace is defined by the set with coefficients of C' , D' and d' having the values of C , D and d in Equation 13. The values of C'' , D'' , and d'' for $\mathcal{F}_{0,0}^3$ are,

$$C'' = \begin{bmatrix} 2 & 0 & -1 & 0 \end{bmatrix}, \quad D'' = \begin{bmatrix} 0 \end{bmatrix}, \quad d'' = \begin{bmatrix} 0 \end{bmatrix} \quad (18)$$

because saturating the constraint c_2 on the (3)-face at \mathcal{F}_0^3 (i.e., node $\{3\}$) is what takes us to the (2)-face at $\mathcal{F}_{0,0}^3$ (i.e., node $\{2, 3\}$). Note that the values appearing in Equation 18 are precisely the values from C , D , and d that differ between Equations 5 and 13 (i.e., the coefficients of this additionally saturated constraint c_2).

2.6 Labeling the faces

As simplification proceeds down the face lattice, the choice of the reuse vector ρ at a particular face \mathcal{F}_i^k (from Definition 2.1) influences how the points on each of its child $\mathcal{F}_{i,j}^k$ faces contribute. Let ρ_i^k be the reuse vector selected at \mathcal{F}_i^k . There are three possibilities,

- (1) $\rho_i^k \cdot v_{i,j}^k > 0 \implies$ points on $\mathcal{F}_{i,j}^k$ must contribute via the \oplus operation
- (2) $\rho_i^k \cdot v_{i,j}^k < 0 \implies$ points on $\mathcal{F}_{i,j}^k$ may contribute via the *inverse* \ominus operation
- (3) $\rho_i^k \cdot v_{i,j}^k = 0 \implies$ points on $\mathcal{F}_{i,j}^k$ have no additional contribution

where $v_{i,j}^k$ is the normal vector of the additionally saturated constraint on $\mathcal{F}_{i,j}^k$ from Definition 2.3. We will say each of the $\mathcal{F}_{i,j}^k$ child faces can be *labeled* as either a \oplus -face, \ominus -face, or \emptyset -face respectively and that the choice of ρ *induces* a particular combination of labels on the facets. This is illustrated in Figure 7.

Each $\mathcal{F}_{i,j}^k$ is classified as a strong or weak boundary facet based on the following definitions.

Definition 2.5. Let $\mathcal{F}_{i,j}^k$ be called a *strong* boundary facet if the following condition holds,

$$\text{rank}(A \cap \mathcal{H}_j^{k-1}) = \text{rank}(A) \quad (19)$$

where $A = \ker(f_p)$ is the accumulation space defined previously in Equation 8.

Definition 2.6. Let $\mathcal{F}_{i,j}^k$ be called a *weak* boundary facet if the following condition holds,

$$0 < \text{rank}(A \cap \mathcal{H}_j^{k-1}) < \text{rank}(A) \quad (20)$$

Boundary faces are useful because they only contribute via the \oplus operation. Those boundary faces that are also labeled as \ominus -faces can be ignored because they do not contribute to any element of the output. This is what we saw with the vertical blue edge in Figure 4.

Each $\mathcal{F}_{i,j}^k$ is further classified as a strong or weak invariant facet based on the following definitions. This is the dual of the boundary definitions, from the perspective of the dependence function, f_r .

Definition 2.7. Let $\mathcal{F}_{i,j}^k$ be called a *strong* invariant facet if the following condition holds,

$$\text{rank}(\ker(f_r) \cap \mathcal{H}_j^{k-1}) = \text{rank}(\ker(f_r)) \quad (21)$$

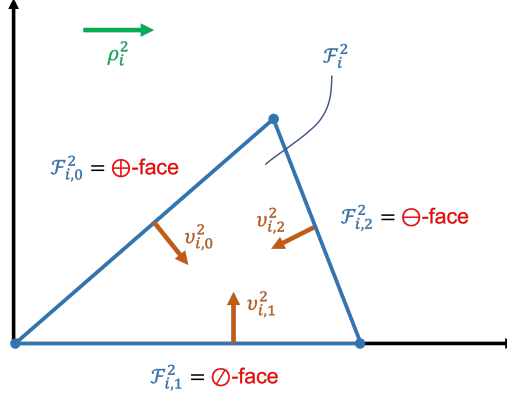


Fig. 7. Illustration of the influence of the choice of reuse vector ρ on how points on child facets contribute. Suppose that this triangular (2)-face, denoted as \mathcal{F}_i^2 , exists in the face lattice. It has three (1)-faces (i.e., 3 edges) and the normal vectors, $v_{i,0}^2$, $v_{i,1}^2$, and $v_{i,2}^2$ for each, point inward as shown. If ρ_i^2 is chosen as drawn here (a vector in this plane and pointing to right), then the points in the $\mathcal{F}_{i,0}^2$ face, for example, contribute via the \oplus operation because $\rho_i^2 \cdot v_{i,0}^2 > 0$.

Definition 2.8. Let $\mathcal{F}_{i,j}^k$ be called a *weak invariant facet* if the following condition holds,

$$0 < \text{rank}(\ker(f_r) \cap \mathcal{H}_j^{k-1}) < \text{rank}(\ker(f_r)) \quad (22)$$

As with strong boundary facets, the property that make strong *invariant* facets significant is that their points never contribute in the residual computation regardless of the reuse vector chosen. This is because any reuse vector in the reuse space is also in the linear space \mathcal{H}_j^{k-1} of the facet.

2.7 Reduction Decomposition

Because the reduction operator is commutative, we may have multi-dimensional accumulations, and it is possible to carry out the accumulation in a particular order as discussed by Gautam and Rajopadhye [2006] with the transformation called “reduction decomposition.” Given a reduction of the form in Equation 6, it is always possible to rewrite it as the following two reductions,

$$Y[f_p''(z)] = \bigoplus_{z \in \mathcal{D}} Z[f_p'(z)] \quad (23)$$

$$Z[f_p'(z)] = \bigoplus_{z \in \mathcal{D}} X[f_r(z)] \quad (24)$$

with the introduction of a new variable Z to hold partial answers, for any two functions f_p'' and f_p' such that $f_p = f_p'' \circ f_p'$. We can think of this as decomposing a higher dimensional reduction into a lower dimensional *reduction of reductions*. This is always legal since the order of accumulation in any particular reduction does not matter, by definition. This is useful because any facet that is characterized as a weak boundary per Definition 2.6 can be characterized as a strong boundary facet by appropriately choosing f_p' . We rely heavily on this transformation and a concrete example is provided in the solution for Exercise 3 discussed in Section 6.

Also note that any split is legal in the sense that for any disjoint \mathcal{D}_1 and \mathcal{D}_2 such that $\mathcal{D} = \mathcal{D}_1 \cup \mathcal{D}_2$, the reduction in Equation 6 can be rewritten as the following,

$$Y[f_p(z)] = \begin{cases} f_p(\mathcal{D}_1) \cap f_p(\mathcal{D}_2) & : \left(\bigoplus_{z \in \mathcal{D}_1} X[f_r(z)] \right) \oplus \left(\bigoplus_{z \in \mathcal{D}_2} X[f_r(z)] \right) \\ f_p(\mathcal{D}_1) \setminus f_p(\mathcal{D}_2) & : \bigoplus_{z \in \mathcal{D}_1} X[f_r(z)] \\ f_p(\mathcal{D}_2) \setminus f_p(\mathcal{D}_1) & : \bigoplus_{z \in \mathcal{D}_2} X[f_r(z)] \end{cases} \quad (25)$$

Note that the result is defined over three distinct regions based on the intersection and difference of the projections of the domains \mathcal{D}_1 and \mathcal{D}_2 . The reader can refer to Le Verge [1992b] for the proof and additional information.

2.8 Feasible reuse space

The residual computations are used in the following way.

- The boundary \oplus -faces are used to initialize the final answer.
- The values on non-boundary \oplus -faces are combined with $Y[f_p(z - \rho)]$ using \oplus .
- The results of \ominus -face non-boundary faces are combined with $Y[f_p(z - \rho)]$ using \ominus .

The reason that simplification may fail is because it may not be possible to choose a reuse vector ρ where either $\mathcal{F}' \setminus \mathcal{F}$ or $\mathcal{F} \setminus \mathcal{F}'$ is empty (i.e., all possible choices of ρ may induce at least one pair of opposing \ominus -face and \oplus -face labels on two of the facets). We will need to reason about the reuse space at a particular (k)-face, \mathcal{F}_i^k , in the face lattice. Each facet $\mathcal{F}_{i,j}^k$ of \mathcal{F}_i^k constrains the reuse space if it is not a strong boundary facet based on the definition in Section 2.6.

Let Υ_i^k be the matrix containing the normal vectors $v_{i,j}^k$ of $\mathcal{F}_{i,j}^k$ that are not strong boundary facets. If there are q non-strong boundary facets, then Υ_i^k has the form,

$$\Upsilon_i^k = \begin{bmatrix} v_{i,0}^k \\ v_{i,1}^k \\ \vdots \\ v_{i,q-1}^k \end{bmatrix}$$

When the operator \oplus does not admit an inverse, we call a candidate reuse vector feasible if it labels all facets as \oplus -faces or \emptyset -faces, i.e., any ρ such that $\Upsilon_i^k \rho \geq 0$ is feasible. Alternatively, if a reuse vector labels all facets as \ominus -faces or \emptyset -faces, then the negation of this reuse vector is obviously feasible. However, there cannot be both. Therefore, we define the feasible reuse space to include the case where all facets are \ominus -faces or \emptyset -faces to simplify the proofs in later sections. Let \hat{R}_i^k denote the *feasible reuse space* of \mathcal{F}_i^k and be defined as,

$$\hat{R}_i^k = R \cap (\{\rho \mid \Upsilon_i^k \rho \geq 0\} \cup \{\rho \mid \Upsilon_i^k \rho \leq 0\}) \quad (26)$$

For example, let us construct the feasible reuse space of the reductions given in the first two exercises to quantify why simplification is possible for Exercise 1 but not for Exercise 2. Both examples have the same 2D triangular domain $\mathcal{D} = \{[i, j] \mid i \leq N \text{ and } i \leq j \leq 2i\}$ with the same indexing expression in the reduction body, $f_r : \{[i, j] \rightarrow [j]\}$, and therefore the same 1D reuse space per Equation 10,

$$R = \ker(f_r) = \{[i, j] \mid j = 0\} \quad (27)$$

Similarly, both use the same projection function $f_p : \{[i, j] \rightarrow [i]\}$ and therefore have the same 1D accumulation space per Equation 8,

$$A = \ker(f_p) = \{[i, j] \mid i = 0\} \quad (28)$$

The three constraints of \mathcal{D} are shown in Figure 8 along with their corresponding normal vectors,

j	c_j	v_j	\mathcal{H}_j	$\mathcal{H}_j \cap A$	$\text{rank}(\mathcal{H}_j \cap A)$	Classification
0	$-i + N \geq 0$	$[-1, 0]$	$\{[i, j] \mid i = 0\}$	$\{[i, j] \mid i = 0\}$	1	boundary
1	$-i + j \geq 0$	$[-1, 1]$	$\{[i, j] \mid i = j\}$	$\{[0, 0]\}$	0	non-boundary
2	$2i - j \geq 0$	$[2, -1]$	$\{[i, j] \mid 2i = j\}$	$\{[0, 0]\}$	0	non-boundary

Fig. 8. Constraints c_j characterizing the facets of the domain \mathcal{D} of the reduction bodies for Exercises 1 and 2. Each row is a facet of \mathcal{D} . Each facet's normal vector (per Definition 2.3) and linear subspace (per Definition 2.4) are shown by v_j and \mathcal{H}_j respectively.

linear subspaces, and classifications as either boundary or non-boundary facets according to Definition 2.5. The facet with $i = N$ is a boundary because its linear subspace contains the entire accumulation space (i.e., its intersection with the 1D accumulation space *remains* a 1D space).

Now, for Exercise 1 the reduction operator is addition which admits an inverse so the feasible reuse space is just R shown in Equation 27. However, for Exercise 2, since the max operator does not admit an inverse, we must further constrain R according to Equation 26. Here, Υ is constructed from the two non-boundary facets v_1 and v_2 as,

$$\Upsilon = \begin{bmatrix} -1 & 1 \\ 2 & -1 \end{bmatrix} \quad (29)$$

which gives the following empty³ feasible reuse space \hat{R} ,

$$\hat{R} = \{[i, j] \mid j = 0\} \cap (\{[i, j] \mid i \leq j \text{ and } j \leq 2i\} \cup \{[i, j] \mid i \geq j \text{ and } j \geq 2i\}) = \{[0, 0]\}$$

Since the only possible reuse vector that can be chosen is the zero vector, simplification fails.

3 PROBLEM FORMULATION AND HYPOTHESES

As we have discussed till now, simplification is a powerful transformation that enables a reduction in the asymptotic complexity of the underlying computation. However, it is not always possible as motivated by Exercise 2. In this section, we present our primary claim in the form of Theorem 3.1 stating it is always possible to exploit all available reuse for any arbitrary reduction even if the feasible reuse space is empty as discussed above.

THEOREM 3.1. *An arbitrary reduction with a d -dimensional body, an a -dimensional accumulation space, and an r -dimensional reuse space can always be transformed into an equivalent reduction with an asymptotic complexity that has been decreased by $l = \min(a, r)$ polynomial degrees⁴.*

The proof of Theorem 3.1 will follow from Sections 4 and 5 where we show how to handle all possible scenarios. We will carefully consider all possible combinations of the dimensionalities of accumulation space, reuse space, and reduction body that can occur. For each case, we show that the reduction can be split into finitely many pieces such that the feasible reuse space of each piece is non-empty, and can therefore be simplified. We make several assumptions about the input

³The reuse space only contains the zero vector, which will call empty from the perspective of being able to choose a reuse vector that can be used for simplification.

⁴A 3D reduction that produces a 2D answer cannot be performed with anything less than quadratic work, even if there are two available dimensions of reuse.

reduction under analysis. This does not introduce any loss of generality, as we explain in the remainder of this section.

Assumption: Orthogonal reuse and accumulation with canonical bases

We make the following assumptions about the relationship between the accumulation space and the reuse space.

- The accumulation and reuse spaces are *orthogonal* and are oriented along a subset of the canonical axes. We let the reuse space be along the first r canonical axes, and the accumulation space be along the last a axes.
- The reduction consists of accumulation and reuse dimensions only, i.e., $a + r = d$.

There is no loss in generality from the first assumption, because the equation (i.e., the domain, the input and out variables, and the indexing expressions) can always be reindexed to achieve them. For example, the counter-intuitive prefix-max of Equation 12 can be massaged into the conventional form below, by simply “aligning” the input variable along the j -axis, and “reversing the accumulation” and appropriately modifying the access functions.

$$Y[i] = \max_{j=0}^i X[j]$$

Regarding the second assumption, first note that reductions with $a + r > d$ represent instances where the accumulation and reuse space have a non-trivial intersection. In these cases, the reduction accumulates multiple instances of the *same value* at many points in the reduction body (i.e., along this intersection). Gautam and Rajopadhye [2006] describe how such reductions can be handled with a higher order operator simplification, which transforms the reduction into one where $a + r = d$. Therefore, we only need to consider reductions where $a + r = d$.

On the other hand, reductions with $a + r < d$ can always be transformed into families of reductions, with $d - (a + r)$ *independent parameters*, reading independent slices of the inputs and producing independent slices of the outputs. For example, suppose we encounter the reduction,

$$Y[i, j] = \max_{k=i}^{2i} X[j, k] \quad (30)$$

It has a 3D domain, 1D accumulation, and 1D reuse space, but if we treat the index j as a parameter, then this can really be viewed as $O(N)$ instances of 2D reductions with a 1D accumulation and 1D reuse space, one for each value of j , embedded in a 3D space. No simplification is possible among the different instances (each of the $O(N)$ reduction instances along j must be computed), but further simplification may be possible within the ik dimensions).

Further at any point down the face lattice, if we encounter a residual reduction where $a + r \neq d$, it can be preprocessed to recover a reduction of the form $a + r = d$ as discussed in Section 3.2

Assumption: Simplicial domains

In our proofs, we restrict the domains of the reduction body to simplicial (or hyper-triangular) domains, defined as follows.

Definition 3.2. A (d) -simplex is the (d) -dimensional polytope defined as the convex combination of any $d + 1$ linearly independent vertices.

The maximal simplification result directly carries over to general convex polyhedral sets, because any (d) -dimensional parametric polytope can be decomposed into the union of (d) -dimensional simplices with a finite number of splits [Edmonds 1970]. If any non-simplicial domain is constructed during simplification, it is decomposed into simplices. Note that the Integer Set Library supports enumerating parametric vertices by splitting parametric polyhedra into chambers. A chamber is a

subset of the parameter space where the polyhedra in this subdomain exhibit homothetic scaling. For each chamber, the number of vertices and their relative positions do not change, and thus the simplicial decomposition for non-parametric polyhedra from Edmonds [1970] can be applied. Simplices have useful properties used in our proofs:

- Any (k) -face of an (d) -simplex is itself a (k) -simplex. This is because the number of (k) -faces of a (d) -simplex are given by the binomial coefficients, $\binom{d+1}{k+1}$ unique combinations of its $d+1$ vertices.
- Any (d) -simplex can be always be split into two (d) -simplices with the addition of one new linearly independent vertex.

3.1 Maximal Simplification Algorithm

Given an input reduction in the form of Equation 6, the high-level algorithm for maximal simplification is summarized as follows:

- (1) decompose the input domain into simplices and process each one separately
- (2) for each simplex, construct its face lattice and do the following starting from the root node in the lattice
- (3) run the Gautam and Rajopadhye [2006] algorithm and try to identify a candidate reuse vector at the current node in the lattice, using reduction decomposition as necessary
- (4) if a reuse vector can be found then apply the Gautam and Rajopadhye [2006] simplification transformation to reduce the asymptotic complexity by one degree
- (5) if the Gautam and Rajopadhye [2006] algorithm fails, recursively split the node into pieces, and continue processing each piece separately
- (6) preprocess to ensure that any residual reductions involve only accumulation and reuse dimensions
- (7) if there is still available reuse and accumulation, recurse into the applicable facets and go to step 3

For reductions with $d \geq 3$, Step 5 can ***always be done with a finite number of splits***, but when $d = 2$ (i.e., for triangular faces) a finite number of splits may not be possible. However, we show that here, with exactly two cuts, its is possible to expose a ***a common repeating pattern***. To complete our proof, we develop an algorithm called *fractal simplification* so that the results can be computed with $O(N)$ work. Sections 4 and 5 describe this more detail.

3.2 Recursive Invariant

Simplification proceeds recursively down the face lattice of the domain of the reduction body. At each face, the following invariant can be maintained:

$$d = a + r \quad (31)$$

At each node \mathcal{F}_i^k in the face lattice, choosing a reuse vector results in residual reductions on the facets $\mathcal{F}_{i,j}^k$. The dimensionality d' of the reductions over the facets is $d' = d - 1$ because there is one less free dimension in each facet by definition. Similarly, the dimensionality of the remaining reuse space is $r' = r - 1$ because we have exploited one dimension of available reuse at the current node. The dimensionality of the accumulation space in each facet depends on whether or not the particular facet is a strong boundary.

If the facet is a strong boundary then it contains the entire accumulation space by Definition 2.5. Therefore the dimensionality of the residual accumulation space is $a' = a$. In this case, the invariant $d' = a' + r'$ still holds. If the facet is a weak boundary, then the dimensionality of the residual accumulation space $a' = a - 1$ decreases by one in the facet. In this case, the residual reduction is

one where $d' > a' + r'$. However, this is really just a series of independent reductions. If we view the independent dimension as a parameter then the invariant still holds. Note that this series of independent reductions may not be simplicial, and may need to be decomposed before the recursion continues. This arises in the simplification of Exercise 3 and is discussed in Section 6.2.6.

4 d-DIMENSIONAL REDUCTIONS

We will look at d -dimensional simplicial domains for $d \geq 3$ first. 2D reductions must be handled specially and are discussed subsequently in Section 5.

To exploit one dimension of reuse, the first thing we do is construct the feasible space of reuse as described in Section 2.8. If this is non-empty, then no further *new* analysis is needed. Simplification proceeds exactly as described in Section 2.3. However, if the feasible space of reuse is empty then we must decide how to split to domain.

LEMMA 4.1. *Let a splitting hyperplane of a (d) -dimensional polytope be any $(d - 1)$ -dimensional hyperplane that has points on both sides of the hyperplane. Any splitting hyperplane that saturates a $(d-2)$ -face of a (d) -simplex produces two (d) -simplices.*

PROOF. By definition, an (d) -simplex is the convex combination of $(d + 1)$ vertices. Additionally, every (k) -face is itself a (k) -simplex which is just the simplex formed by the $(k + 1)$ vertices of the (k) -face. Any splitting $(d - 1)$ -dimensional hyperplane that saturates a $(d - 2)$ -face contains its $(d - 1)$ vertices. There are two remaining vertices and these by definition can not be part of the splitting hyperplane. This is because the hyperplane is itself a $(d - 1)$ -simplex and if it contained one of these additional two vertices, then it would saturate an entire $(d - 1)$ -face of the domain. Therefore, we can consider these other two vertices as separate from the hyperplane. We will refer to these as vertex A and vertex B. The convex combination of vertices A and B forms a (1) -simplex (i.e., a (1) -face or 1-dimensional linear subspace that connects the vertices). Let point C, be any point in this (1) -simplex. We can construct the following two new sets.

- (1) The convex combination of the $(d - 1)$ vertices on the $(d - 2)$ -face, vertex A, and point C.
 - (2) The convex combination of the $(d - 1)$ vertices on the $(d - 2)$ -face, vertex B, and point C.
- Then take the set difference of this set with the $(d - 2)$ -face.

Since both are convex combinations of $(d + 1)$ vertices, they are both by definition (d) -simplices. \square

Consider a hyperplane passing through any of the $d - 1$ vertices of a (d) -simplex. The other two vertices are either on the same side or opposite sides in which case the hyperplane is either redundant or it splits the simplex into two disjoint simplices. We call such hyperplanes a “simplicial cut.” A proof that the pieces are in fact simplices is given in Lemma 4.1. Geometrically, a simplicial cut exposes a single new facet in each of the pieces.

However, notice that there are still infinitely many such simplicial cuts. To refine this, let us characterize each facet (\mathcal{F}^{d-1}) of the simplex as either a strong boundary, a strong invariant faces, or an oblique facet.

Definition 4.2. Let a facet be called *oblique* if it is neither a strong boundary nor a strong invariant face. An oblique facet may be a weak boundary or a weak invariant face.

These classifications are mutually exclusive, there is no such thing as an oblique strong invariant facet for example. The accumulation and reuse spaces are orthogonal, therefore no facet can simultaneously be a strong boundary and a strong invariant face. Only oblique faces constrain the space of feasible reuse per Section 2.8. Let us define a *useful* cut as follows,

Definition 4.3. Let a *useful* cut be any simplicial cut that exposes either a new strong boundary face or a strong invariant face.

The consequence of making useful cuts is that each piece has strictly fewer oblique faces. Thus, we only consider useful cuts in the following reasoning.

LEMMA 4.4. *The linear subspace of any $(d - 1)$ -face has a non-trivial intersection with the linear subspace spanned by any two or more canonic axes.*

PROOF. The $(d - 1)$ -dimensional linear subspace describing any $(d - 1)$ -face involves d indices and one equality constraint. The linear subspace spanned by q canonic axes involves d indices and $(d - q)$ equality constraints and is q -dimensional. Their intersection involves $(1 + d - q)$ equality constraints. Therefore it is $(q - 1)$ -dimensional. When $q > 1$, this intersection is non-trivial. \square

LEMMA 4.5. *When the accumulation space has more than one dimension, all oblique faces are simultaneously weak boundary faces. Similarly, when the reuse space has more than one dimension, all oblique faces are simultaneously weak invariant faces.*

PROOF. The proof follows from Lemma 4.4 because the accumulation and reuse space lie on the canonical axes. \square

LEMMA 4.6. *Given p dimensions of accumulation, any set of p oblique faces can be transformed into $p - 1$ strong boundary faces via reduction decomposition.*

PROOF. Let $[\mathcal{F}_0, \mathcal{F}_1, \dots, \mathcal{F}_{k-1}]$ be the list of oblique faces in any arbitrary order. Take the first oblique face, \mathcal{F}_0 , and let A_0 be the intersection between its linear subspace \mathcal{H}_0 and the accumulation space,

$$A_0 = \mathcal{H}_0 \cap \ker(f_p) \quad (32)$$

The reduction can be decomposed into a reduction of reductions, where the inner reduction's accumulation space is precisely this intersection. The consequence of this is that now, along the inner reduction the face \mathcal{F}_0 is now a strong boundary and so, its labeling does not influence the success or failure of simplification because it does not constraint the feasible space of reuse. A_0 is a $(p - 1)$ -dimensional subspace per Lemma 4.4.

Now let A_{p-2} denote the intersection of the first $(p - 1)$ oblique faces and the accumulation space,

$$A_{p-2} = \mathcal{H}_0 \cap \mathcal{H}_1 \cap \dots \cap \mathcal{H}_{p-2} \cap \ker(f_p) \quad (33)$$

A_{p-2} is a $(a - p + 1)$ -dimensional subspace. Since $a = p$, this is a 1D subspace. The inner reduction now has a 1D accumulation space and $p - 1$ of the oblique faces are now strong boundaries. \square

LEMMA 4.7. *If we have k dimensions of reuse, we can construct a non-empty feasible reuse space from any set of k oblique faces by appropriately choosing ρ .*

PROOF. This is the dual of Lemma 4.6. Everything is identical except we use the dependence function f_r instead of the projection function f_p . Take the first oblique face, \mathcal{F}_0 , and let R_0 be the intersection between its linear subspace \mathcal{H}_0 and the reuse space,

$$R_0 = \mathcal{H}_0 \cap \ker(f_r) \quad (34)$$

R_0 is an $(r - 1)$ -dimensional subspace per Lemma 4.4. Any reuse vector $\rho \in R_0$ in this subspace will label \mathcal{F}_0 as an invariant face. Similarly, let R_{k-2} be the intersection of the first $(k - 1)$ oblique faces with the reuse space,

$$R_{k-2} = \mathcal{H}_0 \cap \mathcal{H}_1 \cap \dots \cap \mathcal{H}_{k-2} \cap \ker(f_r) \quad (35)$$

R_{k-1} is a $(r - k + 1)$ -dimensional subspace. Since $r = k$, this is a 1D subspace. Any reuse vector, $\rho \in R_{k-2}$, simultaneously labels the first $(k - 1)$ oblique faces as invariant faces. A reuse vector can always be chosen to make the last remaining k 'th face a \oplus -face with its negation if necessary. \square

Now consider any d -dimensional reduction over an d -dimensional simplicial domain with a dimensions of accumulation and r remaining dimensions of reuse. There are only two possible types of d -simplices that we must consider:

- (1) $d - 1$ or fewer oblique faces and 2 or more strong boundary and strong invariant faces
- (2) d or more oblique faces

Base Case: $d - 1$ or fewer oblique faces

In this case, $a - 1$ oblique faces can be transformed into strong boundary faces per Lemma 4.6. The remaining $d - a$ oblique faces can be satisfied per Lemma 4.7, since $d - a = r$.

General Case: d or more oblique faces

In this case, we can only satisfy up to $d - 1$ of the oblique faces using Lemmas 4.7 and 4.6. The remaining oblique faces may cause the feasible reuse space to be empty. If this is the case, then we split the domain as follows. Let \mathcal{F}^d denote the domain of the current (d)-face and \mathcal{F}_i^{d-2} denote its i 'th grandchild ($d - 2$)-face. Let f be an affine function from $\mathbb{Z}^d \rightarrow \mathbb{Z}^{d'}$ where $d > d' > 1$. Let $f(\mathcal{F}^d)$ and $f(\mathcal{F}_i^{d-2})$ denote the projection, by f , of \mathcal{F}^d and \mathcal{F}_i^{d-2} respectively. The projection of each ($d - 2$)-face lands either on the interior of $f(\mathcal{F}^d)$, or on a facet of $f(\mathcal{F}^d)$.

Definition 4.8. Let a particular ($d - 2$)-face, \mathcal{F}_i^{d-2} be called *covered* under f if its points are mapped to the *interior* of $f(\mathcal{F}^d)$.

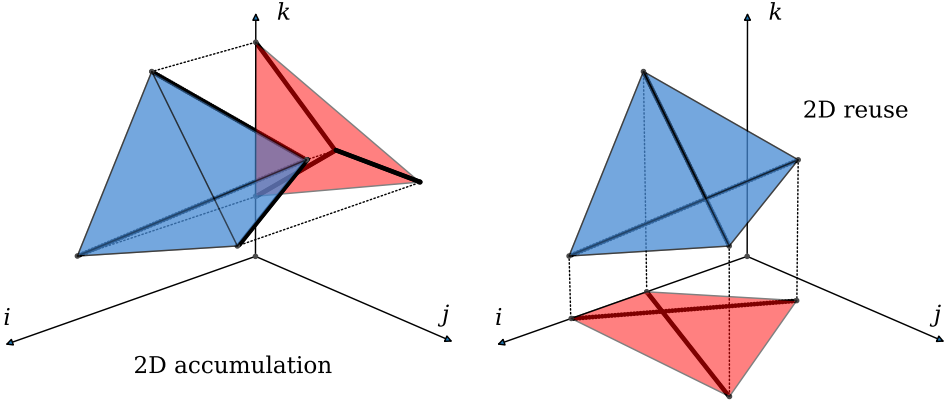


Fig. 9. Covered (1)-simplices (edges) of the blue (3)-simplex (tetrahedron) are shown as the thick black lines depending on which of the accumulation or reuse space is 2-dimensional. The 2D red images are the projection on the canonic axes. We assume that the r -dimensional reuse space is oriented along the first r canonic axes and the a -dimensional accumulation space is along the last a axes. So if the accumulation space is 2D for example, then the reuse space is 1D along the i -axis and the accumulation space is the jk -plane. Conversely, if the reuse space is 2D, then it is the ij -plane and the 1D accumulation space is along the k -axis.

Geometrically, if \mathcal{F}^{d-2} is covered under f then $f(\mathcal{F}^{d-2})$ is a hyperplane that divides $f(\mathcal{F}^d)$ into two non-empty pieces. By extension, any hyperplane that saturates both \mathcal{F}^{d-2} and the null space of f divides \mathcal{F}^d into two non-empty simplices. If f is taken to be either f_p or f_r from Equation 6, characterizing the accumulation and reuse spaces, then any hyperplane through a covered ($d - 2$)-face forms a *useful* cut per Definition 4.3.

An illustration is given in Figure 9 for a 3D example. In 3D either the accumulation space is 2D (and oriented along the last two axes in the jk -plane) or the reuse space is 2D (and oriented along the first two axes in the ij -plane). In this picture, three of the edges become covered if projected onto the jk -plane and two become covered if projected onto the ij -plane. Cuts through these covered edges that expose either new strong invariant or strong boundary facets are useful per Definition 4.3. In Figure 9, there are three possible useful cuts as shown in the left-hand picture. There are two possible useful cuts as shown in the right-hand picture.

LEMMA 4.9. *When there are d or more oblique facets, there must exist at least one $(d - 2)$ -face, \mathcal{F}_i^{d-2} covered by either f_p or f_r .*

PROOF. We will prove this by contradiction. First, note that \mathcal{F}^d has at least d oblique facets, which means there is at most one strong invariant or strong boundary facet. In order for \mathcal{F}_i^{d-2} to not be covered under some function f , its image by f must land in a facet of $f(\mathcal{F}^d)$. Strong boundary facets, when projected onto the reuse space by f_r , land in a facet of $f_r(\mathcal{F}^d)$. Consequently, any of its facets (i.e., $(d - 2)$ -faces of the original \mathcal{F}^d) must also land in a facet of $f_r(\mathcal{F}^d)$. This is due to the fact that the reuse and accumulation spaces are orthogonal. Similarly, strong invariant facets, when projected onto the accumulation space by f_p , land in a facet of $f_p(\mathcal{F}^d)$. Now, let us assume that there are no covered $(d - 2)$ -faces. This means that every parent of each \mathcal{F}_i^{d-2} is either a strong boundary or a strong invariant facet which leads to a contradiction. Therefore, there must be at least one $(d - 2)$ -face covered by either f_p or f_r . \square

When the feasible reuse space of \mathcal{F}^d is empty, a useful cut of \mathcal{F}^d can be constructed as follows. Project the domain onto the accumulation space, and identify a $(d - 2)$ -face that becomes covered. Decompose the projection function to produce an inner reduction with a 1D accumulation space as described in Lemma 4.6. After this decomposition, $a - 1$ of the oblique faces are no longer oblique faces since they are strong boundary faces. Construct the splitting hyperplane as the linear combination of the $(d - 2)$ -dimensional basis of the covered edge and the 1D accumulation space of the inner reduction. Together, this forms a $(d - 1)$ -dimensional basis for a useful splitting hyperplane. This split produces two pieces, each with one fewer oblique face. If there were d oblique faces, then this takes us to the base case. Otherwise, there were $d + 1$ oblique faces, in which case one more cut is needed to take us to the base case.

With this, we have shown that it is always possible to exploit one dimension of reuse at any d -dimensional face. Simplification continues to recurse down the lattice until there are no more available dimensions of reuse.

5 2D REDUCTIONS: FRACTAL SIMPLIFICATION OF TRIANGLES

In 2D, there is only one type of reduction to consider; reductions with a 1D accumulation and 1D reuse space. We will use the words “triangle”, “edge”, and “vertex” instead of “(2)-simplex”, “(1)-face”, and “(0)-face” respectively. Let us assume that the reuse space is oriented horizontally along the i -axis and accumulation vertically along the j -axis. This means that vertical or horizontal edges are, respectively, boundary and invariant edges.⁵ Also note that a *useful* 2D cut, per Definition 4.3, corresponds to *vertical or horizontal cuts through vertices*. Any vertical cut introduces a new boundary and any horizontal cut introduces a new invariant edge.

Now there are only three types of triangles that can occur:

- (1) 1 oblique edge (i.e., a right triangle, which is easy)
- (2) 2 oblique edges (some sub-cases are easy, and the others requires fractal simplification)

⁵The distinction between *strong* and *weak* faces only has meaning in 3D or higher, so we omit that qualification.

- (3) 3 oblique edges, (can be easily split into two disjoint instances of (2))

5.1 Base Case: right triangles

Any triangle with only one oblique edge can always be simplified. If the oblique edge is monotonically increasing, we exploit reuse along $\langle 1, 0 \rangle$. This yields a standard scan (e.g., prefix-max, prefix-min etc.) Otherwise, we exploit reuse along $\langle -1, 0 \rangle$, producing a backward scan (suffix-max, suffix-min etc.)

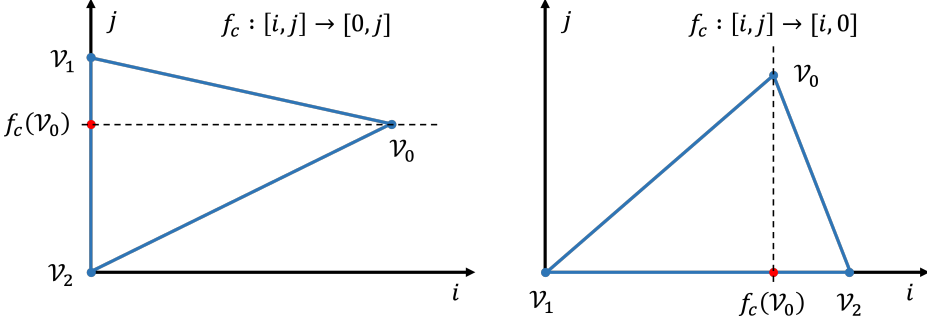


Fig. 10. Covered corner vertex: The projection of \mathcal{V}_0 (shown by the red point) is between \mathcal{V}_1 and \mathcal{V}_2 . A single horizontal or vertical cut through the corner produces two right triangles.

5.2 Two oblique edges

In this case there is either one boundary (vertical) or one invariant (horizontal) edge. Let the three vertices of the triangle be, $\{\mathcal{V}_0, \mathcal{V}_1, \mathcal{V}_2\}$, of which, \mathcal{V}_0 , which we call the corner vertex, is the intersection of the two oblique edges. There are two sub cases depending on whether or not it is covered.

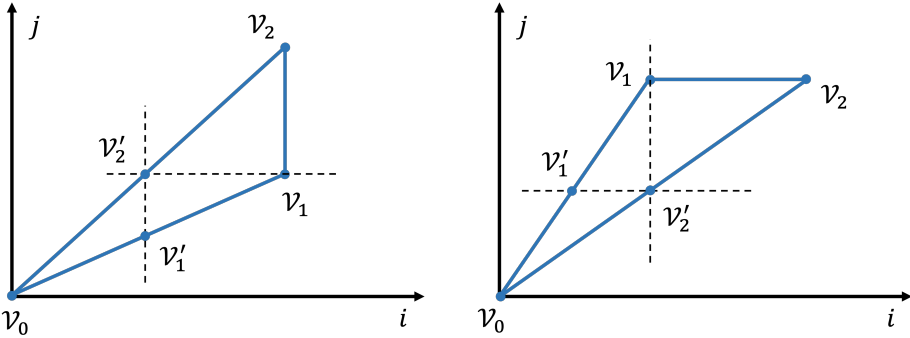


Fig. 11. Non-covered corner vertex: \mathcal{V}_0 lands *outside* of the other two vertices when projected onto the linear space of the vertical edge (left) or when projected onto the space of the invariant edge (right). Each case requires a single vertical and horizontal cut to produce two good right triangles in the base and a third triangle which is a homothetic scaling of the original triangle.

5.2.1 Covered corner. As illustrated by the red point in Figure 10, and by the definition of \mathcal{V}_0 being covered, its projection on the other edge is a point on that edge. Hence a useful cut through \mathcal{V}_0 yields two right triangles. One of them can be simplified as a forward-scan and the other one as a backward-scan.

5.2.2 Corner vertex is not covered. There is no loss of generality in assuming that the entire triangle is in the positive quadrant, and the corner is at the origin (this can be accomplished by a simple reversal of one or both of the input/output arrays). Let us first consider that the non-oblique edge is vertical, and let \mathcal{V}_1 be below \mathcal{V}_2 . If n is sufficiently large, we make one horizontal cut through the lower vertex, \mathcal{V}_1 , and let \mathcal{V}'_2 be its intersection with the upper oblique edge. Next, we make a vertical cut through \mathcal{V}'_2 , intersecting the lower oblique edge at, say \mathcal{V}'_1 . We now have three triangles, $\Delta_1 = [\mathcal{V}_0, \mathcal{V}'_1, \mathcal{V}'_2]$, $\Delta_2 = [\mathcal{V}'_1, \mathcal{V}'_2, \mathcal{V}_1]$ and $\Delta_3 = [\mathcal{V}'_2, \mathcal{V}_1, \mathcal{V}_2]$. Of these the latter two are right triangles, and Δ_1 is a homothetic scaling down of the original triangle as illustrated on the left side of Figure 11.

THEOREM 5.1. *The reduction over $[\mathcal{V}_0, \mathcal{V}_1, \mathcal{V}_2]$ can be simplified, i.e., computed with $O(1)$ reduction operations per element of the answer variable Y .*

PROOF. By Induction. As the base case, consider $n \leq c$, for some constant c . For such sufficiently small triangles, computing each element of Y needs only $O(1)$ reduction operations. In general, when n is sufficiently large, let us assume by induction that Δ_1 can be simplified to compute the section of the result until \mathcal{V}'_1 in $O(1)$ time per element of Y . Another backward scan, and a forward scan on appropriate section of X , will yield the next section of Y from \mathcal{V}'_1 to \mathcal{V}_1 . \square

The above argument can be carried over mutatis mutandis to the case where the non-oblique edge is horizontal. Indeed, as illustrated on the right side of Figure 11, the first cut of the previous case yields the second one.

The proof of Theorem 5.1 suggests a simple code generation strategy (again, explained for the case when the non-oblique edge is vertical). Note that vertices \mathcal{V}_1 and \mathcal{V}_2 are given as affine functions of the parameter, n , and this is known statically. Let $\mathcal{V}_1 = [an, bn]$ and $\mathcal{V}_2 = [an, b'n]$ for some scalars a, b and b' . Using simple grade school geometry (similarity of triangles), we can compute the values of a_1, b_1 and b'_1 the factors that specify \mathcal{V}'_1 and \mathcal{V}'_2 , and from that, the scaling factor, $\frac{a}{a_0} = \frac{b}{b_0} = \frac{b'}{b'_0}$. This leads to the code structure shown in Figure 12. It is important to note that this code is recursive, not polyhedral, and takes us out of the polyhedral model. Nevertheless, all our analyses are polyhedral, and in order to generate it, we need only a fixed number of splits. Also, note that the recursive function calls can be optimized using standard tail recursion optimization techniques.

Case 2: three oblique edges

In this case any vertical cut through a covered vertex when projected onto the i -axis will produce two triangles in case 2. Alternatively, and equivalently, any horizontal cut through a covered vertex when projected on the j -axis will achieve the same thing.

6 SOLUTIONS TO THE EXERCISES

In this section we provide the solutions to the exercises given in Section 1. We intend to include the complete working code for each exercise as an accompanying artifact⁶.

⁶Complete solutions to the exercises can be found at <https://github.com/lnarmour/max-simplification-artifact>

```

void fractal(int *Y, int *X, int L, int U) {
    if (U < threshold) { // do the original O(N^2) reduction
        for (i=L; i<U; i++)
            for (j=i; j<=2*j; j++)
                Y[i] = max(Y[i], X[j]);
        return;
    }
    for (i=U; i>=U/2; i--) // backward scan on U/2<=i<=U
        Y[i] = max(Y[i+1], X[i]);
    for (i=U/2; i<=U; i++) // forward scan on U/2<=i<=U
        Y[i] = max(Y[i-1], X[2*i], X[2*i-1]);
    fractal(Y, X, L, U/2); // recurse on L<=i<U/2
}

```

Fig. 12. Recursive pseudo-code for fractal simplification.

6.1 Exercises 1 and 2

The first exercise is completely handled by the simplification algorithm from Gautam and Rajopadhye [2006] since the reduction operator, addition in this case, admits an inverse. Given the equation of Exercise 1 and the reuse space R , which we previously showed how to construct, in Equation 27, let us select the reuse vector $\rho = [1, 0] \in R$. This induces the labels on the facets as shown in

j	c_j	v_j	Classification	$\rho \cdot v_j$	label
0	$-i + N \geq 0$	$[-1, 0]$	boundary	<0	\ominus -face
1	$-i + j \geq 0$	$[-1, 1]$	non-boundary	<0	\ominus -face
2	$2i - j \geq 0$	$[2, -1]$	non-boundary	>0	\oplus -face

Fig. 13. Showing how the choice of $\rho = [1, 0]$ labels the facets of the reduction body of Exercise 1 as discussed in Section 2.6.

Figure 13. The boundary facet labeled as an \ominus -face can be ignored since it does not contribute to any answer leaving a single \oplus -face on the top oblique edge and a single \ominus -face on the bottom oblique edge. Using the rules in Section 2.8, we can rewrite the equation for Exercise 1 as,

$$Y[i] = \begin{cases} X[0] & i = 0 \\ Y[i-1] + X[2i] + X[2i-1] - X[i-1] & i > 0 \end{cases} \quad (36)$$

Exercise 2 has the same structure except the feasible reuse space is empty as shown in Equation 29. In this case, we must follow the procedure outlined in Section 5. Note that Exercise 2 is precisely the triangle shown on the left of Figure 11 and the recursive code given in Figure 12 illustrates the solution.

6.2 Exercise 3

Let us first express Exercise 3 in the following form,

$$Y[i, j] = \max_{[i, j, k, l] \in \mathcal{D}} X[k, l]$$

$$Y[f_p(z)] = \max_{z \in \mathcal{D}} X[f_r(z)] \quad (37)$$

where $f_p = \{[i, j, k, l] \rightarrow [i, j]\}$ and $f_r = \{[i, j, k, l] \rightarrow [k, l]\}$ with the domain \mathcal{D} as defined in Equation 11 shown again,

$$\mathcal{D} = \{[i, j, k, l] \mid j \leq N \text{ and } i \leq k \leq 2i \text{ and } i + j \leq l \leq 2j\}$$

<pre> for (i=0; i<=N; i++) for (j=i; j<=N; j++) for (l=i+j; l<=2*j; l++) for (k=i; k<=2*i; k++) Z(i,j,l) = max(Z(i,j,l), X(k,l)); for (i=0; i<=N; i++) for (j=i; j<=N; j++) for (l=i+j; l<=2*j; l++) Y(i,j) = max(Y(i,j), Z(i,j,l)); </pre> <p>Decomposition puts inner accumulation along k.</p>	<p>A</p>	<pre> for (i=0; i<=N; i++) for (j=i; j<=N; j++) { for (l=i+j; l<2*j-1; l++) Z(i,j,l) = Z(i,j-1,l); for (l=max(2*j-1,i+j); l<=2*j; l++) for (k=i; k<=2*i; k++) Z(i,j,l) = max(Z(i,j,l), X(k,l)); } for (i=0; i<=N; i++) for (j=i; j<=N; j++) for (l=i+j; l<=2*j; l++) Y(i,j) = max(Y(i,j), Z(i,j,l)); </pre> <p>Exploit one dimension of reuse. Note this now has cubic complexity.</p>	<p>B</p>	<pre> for (i=0; i<=N; i++) for (j=i; j<=N; j++) for (k=i; k<=2*i; k++) for (l=max(2*j-1,i+j); l<=2*j; l++) Z(i,j,l) = max(Z(i,j,l), X(k,l)); for (i=0; i<=N; i++) { Y(i,i) = Z(i,i,2*i); for (j=i+1; j<=N; j++) for (l=i+j; l<=2*j; l++) Y(i,j) = max(Y(i,j), Z(i,(l+1)/2,l)); } </pre> <p>Z is cubic, but only values on some of its facets are actually used.</p>	<p>C</p>	<pre> #define Y_outer(i,l) Z(i,(l+1)/2,l) for (l=0; l<=2*N+2; l++) for (i=0; i<=l/2; i++) for (k=i; k<=2*i; k++) Y_outer(i,l) = max(Y_outer(i,l), X(k,l)); for (i=0; i<=N; i++) { for (k=i; k<=2*i; k++) Y(i,i) = max(Y(i,i), X(k,2*i)); } for (i=0; i<=N; i++) for (j=i+1; j<=N; j++) for (l=i+j; l<=2*j; l++) Y(i,j) = max(Y(i,j), Y_outer(i,l)); </pre> <p>Cast as 3D reductions with 1D accumulation and 1D reuse.</p>	<p>D</p>	<pre> #define A(i) Y_outer(i,l) #define B(k) X(k,l) for (l=0; l<=2*N+2; l++) { for (i=0; i<=l/2; i++) for (k=i; k<=2*i; k++) A(i) = max(A(i), B(k)); } #undef A #undef B for (i=0; i<=N; i++) for (k=i; k<=2*i; k++) Y(i,i) = max(Y(i,i), X(k,2*i)); #define A(j) Y(i,j) #define B(l) Y_outer(i,l) for (i=0; i<=N; i++) { for (j=i+1; j<=N; j++) for (l=i+j; l<=2*j; l++) A(j) = max(A(j), B(l)); } #undef A #undef B </pre> <p>Cast as series of independent 2D reductions each with 1D reuse.</p>	<p>E</p>	<pre> #define A(i) Y_outer(i,l) #define B(k) X(k,l) for (l=0; l<=2*N+2; l++) fractal_0(Z, X, 0, l/2) #undef A #undef B for (i=0; i<=N; i++) for (k=i; k<=2*i; k++) Y(i,i) = max(Y(i,i), X(k,2*i)); </pre>	<p>F</p>
---	----------	---	----------	---	----------	---	----------	---	----------	---	----------

Fig. 14. Illustration of the simplification procedure for Exercise 3.

and its corresponding face lattice as shown in Figure 6. Note that \mathcal{D} is a (4)-simplex and in this example, the accumulation (A) and reuse (R) spaces are both 2D,

$$A = \{z = [i, j, k, l] \in \mathbb{Z}^4 \mid i = 0 \text{ and } j = 0\} \quad (38)$$

$$R = \{z = [i, j, k, l] \in \mathbb{Z}^4 \mid k = 0 \text{ and } l = 0\} \quad (39)$$

The explanation of Exercise 3 can be separated into six distinct steps, summarized and shown with their corresponding code fragments in Figure 14. Note that in practice, we would not generate code at each step. However, it is instructive to see the concrete loops resulting from the analysis and transformations performed at each step.

6.2.1 Step A - reduction decomposition to put the inner accumulation along k . Since the input reduction domain is already simplicial and we have already constructed the face lattice, the first thing we must do is step 3 from the algorithm given in Section 3.1. Let us first construct the feasible reuse space as we did for the other exercises in Section 2.8. Figure 15 shows the facets of the root node and we can see the only strong-boundary facet is $\mathcal{F}_{0,0}^4$, therefore, the other four facets constrain the feasible reuse space \hat{R}_0^4 , which we can see is empty,

$$\begin{aligned} \hat{R} = \{[i, j, 0, 0]\} \cap (\{[i, j, k, l] \mid i \leq k \leq 2i \text{ and } i + j \leq l \leq 2j\} \\ \cup \{[i, j, k, l] \mid i \geq k \text{ and } k \geq 2i \text{ and } i + j \geq l \text{ and } l \geq 2j\}) = \{[0, 0, 0, 0]\} \end{aligned}$$

q	$\mathcal{F}_{0,q}^4$	$v_{0,q}^4$	$\mathcal{H}_{0,q}^4$	$\mathcal{H}_{0,q}^4 \cap A$	rank	classification
0	$\mathcal{F}_{0,0}^4$	$[0, 1, 0, 0]$	$\{[i, j, k, l] \mid j = 0\}$	$\{[0, 0, k, l]\}$	2	strong-boundary
1	$\mathcal{F}_{0,1}^4$	$[-1, 0, 1, 0]$	$\{[i, j, k, l] \mid i = k\}$	$\{[0, 0, 0, l]\}$	1	weak-boundary
2	$\mathcal{F}_{0,2}^4$	$[2, 0, -1, 0]$	$\{[i, j, k, l] \mid 2i = k\}$	$\{[0, 0, 0, l]\}$	1	weak-boundary
3	$\mathcal{F}_{0,3}^4$	$[-1, -1, 0, 1]$	$\{[i, j, k, l] \mid i + j = l\}$	$\{[0, 0, k, 0]\}$	1	weak-boundary
4	$\mathcal{F}_{0,4}^4$	$[0, 2, 0, -1]$	$\{[i, j, k, l] \mid 2j = l\}$	$\{[0, 0, k, 0]\}$	1	weak-boundary

Fig. 15. Facets $\mathcal{F}_{0,q}^4$ of the root node \mathcal{F}_0^4 in the face lattice for Exercise 3. We use the subscript q here so as not to confuse it with the index name of the second dimension j . Each row is a (3)-face of \mathcal{D} . Each facet's normal vector (per Definition 2.3) and linear subspace (per Definition 2.4) are shown by v and \mathcal{H} respectively. Since the accumulation is 2D, facets that have intersections with A smaller than rank 2 are considered weak-boundaries by Definition 2.5.

Since the feasible reuse space of $\mathcal{F}_{0,0}^4$ is empty, a reduction decomposition can be performed to transform some of its weak boundaries into a strong boundary as discussed in Section 2.7. This is done by rewriting projection function $f_p = f_p'' \circ f_p'$ such that the inner function f_p' has a null space that is precisely $\mathcal{F}_{0,j}^4 \cap A$ for a particular j . Choosing f_p' such that it has a null space along l , then facets $\mathcal{F}_{0,1}^4$ and $\mathcal{F}_{0,1}^2$ will both become strong boundaries. Alternatively, choosing an f_p' with a null space along k then $\mathcal{F}_{0,3}^4$ and $\mathcal{F}_{0,4}^2$ become strong boundaries. Ultimately, either of these two choices will work and the Gautam and Rajopadhye [2006] algorithm explores all possible decompositions with dynamic programming, but we will only illustrate the second one which puts the inner accumulation along k . Note that any other choice, with a null space along some linear combination of the k and l basis vectors, will not transform any of the weak boundaries into a strong boundary.

Using f_p' and f_p'' as,

$$f_p' = \{[i, j, k, l] \rightarrow [i, j, l]\} \quad (40)$$

$$f_p'' = \{[i, j, l] \rightarrow [i, j]\} \quad (41)$$

puts the inner accumulation along the k dimension (i.e., $\ker(f_p')$ is spanned by the unit vector $[0, 0, 1, 0]$). With this we can rewrite Equation 37 as,

$$Z[i, j, l] = \max_{z \in \mathcal{D}} X[k, l] \quad (42)$$

$$Y[i, j] = \max_{z \in \mathcal{D}} Z[i, j, l] \quad (43)$$

The corresponding loops are shown in box A of Figure 14.

6.2.2 Step B - simplification of the inner reduction. Under this choice of f'_p , the inner reduction, in Equation 42, has the 1D accumulation space A' ,

$$A' = \{[i, j, k, l] \mid i = 0 \text{ and } j = 0 \text{ and } l = 0\} \quad (44)$$

Note that the domain, and thus the facets, of the inner reduction are unchanged. If we now consider which of these facets are boundaries, we can see that indeed $\mathcal{F}_{0,3}^1$ and $\mathcal{F}_{0,4}^2$ are strong boundaries because they contain the entire (smaller) accumulation space in Equation 44.

q	$v_{0,q}^4$	$\mathcal{H}_{0,q}^4$	$\mathcal{H}_{0,q}^4 \cap A'$	rank	classification
0	[0, 1, 0, 0]	$\{z \mid j = 0\}$	$\{[0, 0, k, 0]\}$	1	strong-boundary
1	[-1, 0, 1, 0]	$\{z \mid i = k\}$	$\{[0, 0, 0, 0]\}$	0	non-boundary
2	[2, 0, -1, 0]	$\{z \mid 2i = k\}$	$\{[0, 0, 0, 0]\}$	0	non-boundary
3	[-1, -1, 0, 1]	$\{z \mid i + j = l\}$	$\{[0, 0, k, 0]\}$	1	strong-boundary
4	[0, 2, 0, -1]	$\{z \mid 2j = l\}$	$\{[0, 0, k, 0]\}$	1	strong-boundary

Fig. 16. Facets $\mathcal{F}_{0,q}^4$ under the inner projection function f'_p in Equation 40 after decomposition.

Now the feasible reuse space (of the inner reduction) is only constrained by $\mathcal{F}_{0,1}^1$ and $\mathcal{F}_{0,2}^2$,

$$\begin{aligned} \hat{R} &= \{[i, j, 0, 0]\} \cap (\{[i, j, k, l] \mid i \leq k \leq 2i\} \cup \{[i, j, k, l] \mid i \geq k \text{ and } k \geq 2i\}) \\ &= \{[0, j, 0, 0]\} \end{aligned}$$

which is non-empty. Choosing the reuse vector $\rho = [0, 1, 0, 0]$, and apply one step of simplification algorithm, we are left with the loops shown in box B of Figure 14. We have not explicitly shown it here but the resulting domains characterizing these loops come from the straightforward application of Theorem 5 from Gautam and Rajopadhye [2006] with the reuse vector $\rho = [0, 1, 0, 0]$. This corresponds to step 4 in Section 3.1.

6.2.3 Step C - recover the residual reductions. Notice that the new variable Z is 3D but it is not necessary to compute all of its values since the value at every *interior* point is identical (i.e., $Z(i, j, l) = Z(i, j - 1, l)$). Only values on the $l = 2j$ facet are needed, leading to the set of loops shown in box C of Figure 14 where the values read from Z in the outer reduction are precisely on this facet when $j = (l + 1)/2$. This corresponds to step 6 in Section 3.1.

6.2.4 Step D - preprocess to cast as series of independent reductions. Since the only values of the inner reduction needed reside on the facet $2j = l$, any reads and writes on $Z(i, j, l)$ can be viewed as reads and writes on some new 2D variable, shown by the macro Y_{outer} in box D of Figure 14, where $j = (l + 1)/2$.

Now the residual 3D reductions can be seen as a series of independent 2D reductions parameterized by some *constant* dimension outlined in the red and green dotted lines in box D of Figure 14. The first series of 2D reductions is parameterized by l and the second series is parameterized by i . This (and the next two steps E and F) correspond to step 6 in Section 3.1.

6.2.5 Step E - cast as series of independent reductions. Since the values of the outer loops l and i are constant from the perspective of the inner 2D reductions respectively, all of the variable accesses here can really be cast as 1D reads or writes. For example, each read on $X(k, l)$ can really be viewed as a read on some new 1D variable $B(k)$ shown by the first B macro in box E of Figure 14.

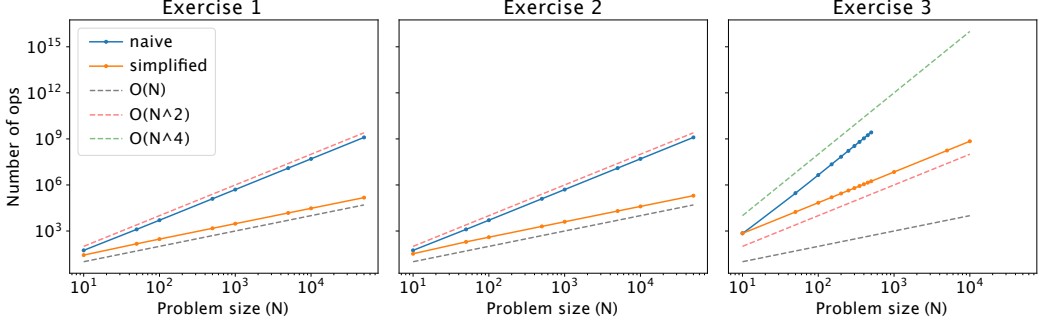


Fig. 17. The naive input reduction is shown in blue and the simplified version in orange. The dotted lines show the corresponding functions N , N^2 , and N^4 respectively. We did not gather data for the naive version of Exercise 3 for large values of N , because the execution time took too long, and we already know what to expect for its behavior.

6.2.6 Step F - Apply recursive simplification. Both series of 2D reductions in box E of Figure 14 have an empty feasible reuse space, which can be seen by building another table like Figure 16, though we do not explicitly show it. The first series, in the red dotted box, has a shape that is precisely the triangle with two oblique edges on the left of Figure 11. Therefore, these loops can be replaced by a call to another function that implements the recursive simplification, denoted as `fractal_0` in box F of Figure 14. The definition of `fractal_0` is not shown here, but it is exactly like that of Figure 12. This corresponds to step 5 in Section 3.1.

Note that the shape of the second series, in the green dotted box, is not simplicial. Before the recursive simplification scheme can be applied, the first iteration of the l loop must be peeled off in order to recover the simplicial domain,

$$[N, i] \rightarrow \{[j, l] : i + 1 \leq j \leq N \text{ and } i + 1 + j \leq l \leq 2j\}$$

where N and now i are treated as parameters. At this point, another recursive simplification can be applied denoted as `fractal_1`. Note that all the loops now have quadratic complexity and there no more available reuse so the simplification procedure terminates successfully. Finally, we have arrived at an implementation that computes the same reduction given in Exercise 3 in $O(N^2)$, which optimally exploits both available dimensions of reuse.

Figure 17 shows a simple plot of the relative performance difference between each exercise and its solution. As expected, the simplification of Exercises 1 and 2 results in $O(N)$ complexity reductions and Exercise 3 in a $O(N^2)$ complexity reduction.

7 CONCLUSIONS AND OPEN QUESTIONS

The ultimate goal is to enable compilers to take a high-level application program specification and carry it out in the most efficient way possible, preferably *automatically* and *optimally*. This work takes a step in that direction to enable users (i.e., application programmers) to focus less on the *engineering* aspects (the *how*) of their algorithms and more on the problems (the *what*) that their algorithms are intended to solve. In this work, we have studied reuse-based simplification of polyhedral reductions. The simplification transformation proceeds recursively down the face lattice of the domain of the reduction body and attempts to exploit one dimension of available reuse at each level. Previously, at some point along this traversal, it may not have been possible to employ the simplification transformation without requiring inverse operations. However, as

we have shown, it is always possible to split the residual reduction at the problematic node in the lattice into a finite number of simplicial pieces in such a way that we can guarantee that the simplification transformation will not fail. We have provided the mathematical proofs which enable us to make this claim.

Our primary claim is that simplification is always possible to enable a reduction in asymptotic complexity. We do not yet have an implementation of the max simplification algorithm as proposed in this work and see this as future work. Since max simplification may result in a residual 2D reduction requiring fractal simplification, this will require a code generation technique outside of the polyhedral model. Along this same line, all of the additional work concerning traditional compile-time scheduling and efficient code generation is still applicable. For example, we rely on the fact that any polyhedral set can be decomposed into a union of disjoint simplices but we do not discuss the implications of the choice of decomposition on the efficiency of the resulting code. It is not obvious at this point in time, for example, why we should prefer one decomposition over another. It may be the case that one particular simplicial decomposition scheme leads to code that is more amenable to vectorization.

These are interesting open questions and this work takes a step toward the holy grail of developing “compilers that invent algorithms.” Exercise 2 was an instance of a program/algorithm, albeit contrived, for which no solution with $O(1)$ time per output value was previously known.

REFERENCES

2006. Prediction of RNA secondary structure by free energy minimization. *Current Opinion in Structural Biology* 16, 3 (2006), 270–278. <https://doi.org/10.1016/j.sbi.2006.05.010> Nucleic acids/Sequences and topology.
- Uday Bondhugula, Vinayaka Bandishti, Albert Cohen, Guillaín Potron, and Nicolas Vasilache. 2014. Tiling and optimizing time-iterated computations over periodic domains. In *2014 23rd International Conference on Parallel Architecture and Compilation Techniques (PACT)*. 39–50. <https://doi.org/10.1145/2628071.2628106>
- Hamidreza Chitsaz, Rolf Backofen, and S.Cenk Sahinalp. 2009a. biRNA: Fast RNA-RNA Binding Sites Prediction. In *Workshop on Algorithms in Bioinformatics (WABI) (LNBI, Vol. 5724)*, S.L. Salzberg and T. Warnow (Eds.). Springer-Verlag, Berlin, Heidelberg, 25–36.
- Hamidreza Chitsaz, Raheleh Salari, S. Cenk Sahinalp, and Rolf Backofen. 2009b. A partition function algorithm for interacting nucleic acid strands. *Bioinformatics* 25, 12 (June 2009), i365–i373.
- Jeffrey Dean and Sanjay Ghemawat. 2008. MapReduce: Simplified Data Processing on Large Clusters. *CACM: Communications of the ACM*. 51, 1 (January 2008), 107–113. <https://doi.org/10.1145/1327452.1327492>
- Allan L Edmonds. 1970. Simplicial decompositions of convex polytopes. *Pi Mu Epsilon Journal* 5, 3 (1970), 124–128.
- P. Feautrier. 1991. Dataflow analysis of array and scalar references. *International Journal of Parallel Programming* 20, 1 (Feb 1991), 23–53.
- Paul Feautrier. 1992a. Some Efficient Solutions to the Affine Scheduling Problem. Part I. One-dimensional Time. *International Journal of Parallel Programming* 21, 5 (1992), 313–347.
- Paul Feautrier. 1992b. Some Efficient Solutions to the Affine Scheduling Problem. Part II. Multidimensional Time. *International Journal of Parallel Programming* 21, 6 (1992), 389–420.
- C. Flamm, W. Fontana, I. L. Hofacker, and P. Schuster. 2000. RNA folding at elementary step resolution. *RNA* 6 (Mar 2000), 325–338.
- J. A. B. Fortes and D. Moldovan. 1984. Data Broadcasting in Linearly Scheduled Array Processors. In *Proceedings, 11th Annual Symposium on Computer Architecture*. 224–231.
- Gautam and S. Rajopadhye. 2006. Simplifying Reductions. In *Conference Record of the 33rd ACM SIGPLAN-SIGACT Symposium on Principles of Programming Languages* (Charleston, South Carolina, USA) (POPL '06). Association for Computing Machinery, New York, NY, USA, 30–41. <https://doi.org/10.1145/1111037.1111041>
- M. Griebel, P. Feautrier, and C. Lengauer. 2000. Index Set Splitting. *IJPP: International Journal of Parallel Programming* 28, 6 (December 2000), 607–631. <https://doi.org/10.1023/A:1007516818651>
- Gautam Gupta, Sanjay Rajopadhye, and Patrice Quinton. 2002. Scheduling Reductions on Realistic Machines. In *Proceedings of the Fourteenth Annual ACM Symposium on Parallel Algorithms and Architectures* (Winnipeg, Manitoba, Canada) (SPAA '02). Association for Computing Machinery, New York, NY, USA, 117–126. <https://doi.org/10.1145/564870.564888>
- F. Irigoin and R. Triolet. 1988. Supernode Partitioning. In *15th ACM Symposium on Principles of Programming Languages*. ACM, 319–328.
- Kenneth E. Iverson. 1962. A Programming Language. In *Proceedings of the May 1-3, 1962, Spring Joint Computer Conference* (San Francisco, California) (AIEE-IRE '62 (Spring)). Association for Computing Machinery, New York, NY, USA, 345–351. <https://doi.org/10.1145/1460833.1460872>
- M. S. Lam. 1989. *A Systolic Array Optimizing Computer*. Kluwer Academic (Springer). <https://doi.org/10.1007/978-1-4613-1705-0> ISBN:-13: 978-14612-8961-6.
- Chris Lattner, Mehdi Amini, Uday Bondhugula, Albert Cohen, Andy Davis, Jacques Pienaar, River Riddle, Tatiana Shpeisman, Nicolas Vasilache, and Oleksandr Zinenko. 2021. MLIR: Scaling Compiler Infrastructure for Domain Specific Computation. In *2021 IEEE/ACM International Symposium on Code Generation and Optimization (CGO)*. IEEE, Seoul, South Korea, 2–14. <https://doi.org/10.1109/CGO51591.2021.9370308>
- Chris Lattner, Jacques A. Pienaar, Mehdi Amini, Uday Bondhugula, River Riddle, Albert Cohen, Tatiana Shpeisman, Andy Davis, Nicolas Vasilache, and Oleksandr Zinenko. 2020. MLIR: A Compiler Infrastructure for the End of Moore’s Law. *CoRR* abs/2002.11054 (2020), 21 pages. arXiv:2002.11054 <https://arxiv.org/abs/2002.11054>
- H. Le Verge. 1992a. Reduction operators in Alpha. In *Parallel Algorithms and Architectures, Europe (LNCS)*, D. Etiemble and J-C. Syre (Eds.). Springer Verlag, Paris, 397–411. See also, Le Verge Thesis (in French).
- H. Le Verge. 1992b. *Un environnement de transformations de programmes pour la synthèse d’architectures régulières*. Ph.D. Dissertation. L’Université de Rennes I, IRISA, Campus de Beaulieu, Rennes, France.
- C. Lengauer. 1993. Loop Parallelization in the Polytope Model. In *CONCUR 93 (Springer-Verlag Lecture Notes in Computer Science, 715)*, E. Best (Ed.). 398–416.
- Guo-Jie Li and Benjamin W. Wah. 1985. Systolic Processing for Dynamic Programming Problems. In *International Conference on Parallel Processing, ICPP’85*. IEEE Computer Society Press, 434–441.
- Vincent Loechner and Doran K. Wilde. 1997. Parameterized Polyhedra and Their Vertices. *IJPP: International Journal of Parallel Programming* 25, 6 (December 1997), 525–549. <https://doi.org/10.1023/A:1025117523902>

- Ronny Lorenz, Stephan H Bernhart, Christian Höner zu Siederdisen, Hakim Tafer, Christoph Flamm, Peter F Stadler, and Ivo L Hofacker. 2011. ViennaRNA Package 2.0. *Algorithms for molecular biology* 6, 1 (2011), 1–14.
- R.B. Lyngso, M. Zuker, and C.N.S. Pedersen. 1999a. Fast evaluation of internal loops in RNA secondary structure prediction. *Bioinformatics* 15, 6 (1999), 440–445.
- R. B. Lyngso, M. Zuker, and C. N. S. Pedersen. 1999b. Fast Evaluation of Internal Loops in RNA Secondary Structure Prediction. *Bioinformatics* 15 (Jun 1999), 440–445.
- R. Nussinov and A. Jacobson. 1980. Fast algorithm for predicting the secondary structure of single stranded RNA. *Proc. Nat. Acad. Sci. USA* 77, 11 (1980), 6309–6313.
- Ruth Nussinov, George Pieczenik, Jerrold R. Griggs, and Daniel J. Kleitman. 1978. Algorithms for Loop Matchings. *SIAM J. Appl. Math.* 35, 1 (1978), 68–82. <https://doi.org/10.1137/0135006>
- P. Quinton and V. Van Dongen. 1989. The Mapping of Linear Recurrence Equations on Regular Arrays. *Journal of VLSI Signal Processing* 1, 2 (1989), 95–113.
- S. V. Rajopadhye. 1986. *Synthesis, Optimization and Verification of Systolic Architectures*. Ph. D. Dissertation. University of Utah, Salt Lake City, Utah 84112.
- S. V. Rajopadhye. 1989. Synthesizing Systolic Arrays with Control Signals from Recurrence Equations. *Distributed Computing* 3 (May 1989), 88–105.
- S. V. Rajopadhye, L. Mui, and S. Kiaei. 1992. Piecewise Linear Schedules for Recurrence Equations. In *VLSI Signal Processing*, V. K. Yao, R. Jain, W. Przytula, and J. Rabbaey (Eds.). IEEE Signal Processing Society, Napa, 375–384.
- S. V. Rajopadhye, S. Purushothaman, and R. M. Fujimoto. 1986. On Synthesizing Systolic Arrays from Recurrence Equations with Linear Dependencies. In *Proceedings, Sixth Conference on Foundations of Software Technology and Theoretical Computer Science*. Springer Verlag, LNCS 241, New Delhi, India, 488–503.
- Xavier Redon and Paul Feautrier. 1994. Scheduling Reductions. In *Proceedings of the 8th International Conference on Supercomputing* (Manchester, England) (ICS '94). ACM, New York, NY, USA, 117–125. <https://doi.org/10.1145/181181.181319>
- V. P. Roychowdhury. 1988. *Derivation, Extensions and Parallel Implementation of Regular Iterative Algorithms*. Ph. D. Dissertation. Stanford University, Department of Electrical Engineering, Stanford, CA.
- Y. Saouter and P. Quinton. 1993. Computability of Recurrence Equations. *Theoretical Computer Science* 114 (1993).
- Nicolas Vasilache, Albert Cohen, and Louis-Noël Pouchet. 2007. Automatic Correction of Loop Transformations. In *16th International Conference on Parallel Architecture and Compilation Techniques (PACT 2007)*. 292–304. <https://doi.org/10.1109/PACT.2007.4336220>
- Sven Verdoolaege. 2016. Presburger Formulas and Polyhedral Compilation. <https://doi.org/10.13140/RG.2.1.1174.6323>
- Michael T. Wolfinger, Andreas, Christoph Flamm, Ivo L. Hofacker, and Peter F. Stadler. 2004. Efficient computation of RNA folding dynamics. *Journal of Physics A: Mathematical and General* 37, 17 (2004), 4731–4741.
- F. C. Wong and Jean-Marc Delosme. 1988. Broadcast Removal in Systolic Algorithms. In *International Conference on Systolic Arrays*. San Diego, CA, 403–412.
- Ningning Xie, Tamara Norman, Dominik Grewe, and Dimitrios Vytiniotis. 2022. Synthesizing optimal parallelism placement and reduction strategies on hierarchical systems for deep learning. *Proceedings of Machine Learning and Systems* 4 (2022), 548–566.
- Cambridge Yang, Eric Atkinson, and Michael Carbin. 2020. Simplifying Multiple-Statement Reductions with the Polyhedral Model. arXiv:2007.11203 [cs.PL]
- Cambridge Yang, Eric Atkinson, and Michael Carbin. 2021. Simplifying Dependent Reductions in the Polyhedral Model. *Proc. ACM Program. Lang.* 5, POPL, Article 20 (jan 2021), 33 pages. <https://doi.org/10.1145/3434301>
- Joseph N Zadeh, Conrad D Steenberg, Justin S Bois, Brian R Wolfe, Marshall B Pierce, Asif R Khan, Robert M Dirks, and Niles A Pierce. 2011. NUPACK: Analysis and design of nucleic acid systems. *Journal of computational chemistry* 32, 1 (2011), 170–173.
- Michael Zuker and Patrick Stiegler. 1981. Optimal computer folding of large RNA sequences using thermodynamics and auxiliary information. *Nucleic Acids Research* 9, 1 (1981), 133–148.